Alma Mater Studiorum · Università di Bologna

School of Science
Department of Physics and Astronomy
Master Degree in Physics

Cosmological and Static Spherically Symmetric Solution to Einstein Equation with an Exponential Scalar Potential

Supervisor:
Prof. Roberto Balbinot

Co-Supervisors:
Dr. Fabio Finelli
Dr. Alessandro Gruppuso

Submitted by:
Cristian Ferrante

Academic Year 2021/2022

Abstract

Exponential potentials can be associated both with expanding and collapsing cosmologies: whereas power-law inflation can be obtained for a nearly flat exponential potential, a stable contracting cosmology (which, by the way, can solve the horizon problem) can be obtained for a negative sufficiently steep exponential potential. Motivated by these results, we study the Einstein equation for a scalar field with an exponential potential in a static and spherically symmetric spacetime. For the same parameters which describe a stable contracting cosmology, we find a non-asymptotically flat black hole and we study its properties.

Contents

Abstract **i**

Introduction **iv**

List of symbols, acronyms and notation **vi**

1 Basics of Cosmology **1**

1.1 The Principles of Cosmology 1
1.2 The Friedmann-Lemaître-Robertson-Walker spacetime 2
1.3 Cosmic fluids 3
1.4 The Friedmann equations 4
1.5 The expansion of the Universe 5
1.5.1 The cosmological redshift 5
1.5.2 The luminosity-distance relation 7
1.5.3 The Hubble law 7

2 Inflationary Cosmology **9**

2.1 The horizon problem 9
2.2 The flatness problem 12
2.3 The shrinking comoving Hubble radius: a possible way out 13
2.3.1 Solution to the horizon problem 14
2.3.2 Solution to the flatness problem 15
2.3.3 Equivalent conditions for inflation 15
2.3.4 Duration of inflation: a minimum estimate 17
2.4 Slow-roll inflation 18

3 Scalar field Cosmology with an exponential potential **22**

3.1 Dynamical equations 23
3.2 One-dimensional phase-space 24
3.2.1 Critical points and stability 24
3.2.2 Qualitative evolution in the phase-space 25
3.3 Two-dimensional phase-space 28

3.3.1 Critical points . . . 29
3.3.2 Stability . . . 30
3.3.3 Qualitative evolution in the phase-space . . . 30
3.4 Final considerations . . . 33
3.5 A "Cosmic No-Hair Theorem" for contracting cosmologies . . . 34
3.5.1 The curvature-free case . . . 35
3.5.2 Curvature . . . 39

4 Static spherically symmetric solution with an exponential potential 40
4.1 Equations of motion and their solution in a static and spherically symmetric spacetime . . . 40
4.1.1 Curvature invariants . . . 43
4.2 Relation to Mann solution . . . 43
4.3 Kruskal extension . . . 44
4.4 Parameter Analysis . . . 47
4.5 Comparison between SSS solution and de Sitter Universe . . . 47
4.6 Comparison between SSS solution and the stable collapsing cosmology 48

5 Conclusions and outlooks 50

Appendix A Connecting inflation to observables: CMB anisotropy 51
A.1 Introduction . . . 51
A.2 Large angular scales . . . 53
A.3 Intermediate angular scales . . . 57
A.4 Small angular scales . . . 60
A.4.1 The Silk damping . . . 61
A.4.2 The finite thickness of the LSS . . . 61
A.4.3 The weak gravitational lensing and the Sunyaev-Zeldovich effect 63
A.5 Conclusions . . . 63

Appendix B About scalar field cosmology with an exponential potential 65
B.1 Autonomous system for a FLRW cosmology with an exponential potential . . . 65

INTRODUCTION

Modern Cosmology is based on three main assumptions: General Relativity, the assumption of isotropy and homogeneity, and a description of main matter constituents as perfect fluids. Observations seem to agree with these principles which are the pillars of the standard Hot Big Bang model to a good approximation. Furthermore, they point in the direction of an almost flat Universe. The Hot Big Bang theory faces several conceptual problems, which are solved in an elegant and effective way by the inflationary theory. It describes an early period of extraordinary rapid and accelerated expansion of the Universe. The simplest framework is the so called Canonical Single Field Slow Roll Inflation (henceforth simply slow roll inflation), where a minimally coupled homogeneous scalar field, i.e. the inflaton, is introduced, on top of the usual Einstein-Hilbert action. So far, slow roll inflation is consistent with observations. However, inflation is not the only possible tool in order to deal with the drawbacks of the Hot Big Bang theory. For example, a solution to the horizon problem is also provided by a contracting universe. In this thesis, we will study scalar field cosmologies where the considered potential has an exponential form: the sign and the slope of the potential determine whether we are dealing with power-law inflation (or in general expanding cosmologies) or with collapsing cosmologies.
In a complementary way, we will study the same Einstein equations for a scalar field with an exponential potential in a static and spherically symmetric spacetime and will discuss the properties of the solutions found.
This work is structured as follows: in chapter 1 we will review the basic concepts of Cosmology, in particular the principles and fundamental equations related to the Standard Cosmological Model. In chapter 2 we will deal with inflationary cosmology. First of all, we will present two of the main problems afflicting the HBB theory, i.e. the horizon problem and the flatness problem. Then we will introduce inflation

and show how it is able to solve them, and we will give a rough estimate about its duration. Finally, we will discuss slow roll inflation. In chapter 3 we present a phase-space analysis of a scalar field cosmology with an exponential potential whose sign is left arbitrary and eventually we will discuss a "cosmic no-hair theorem" for contracting cosmologies. In chapter 4 we solve Einstein equations in a static and spherically symmetric spacetime for a cosmology featured by an exponential potential for the scalar field and we will discuss the properties of our solution. Finally, in chapter 5 we will outline the conclusions and possible future outlooks.

LIST OF SYMBOLS, ACRONYMS AND NOTATION

Acronyms

BBN Big Bang Nucleosynthesis

CHR Comoving Hubble Radius

CMB Cosmic Microwave Background

dS de Sitter

EM Energy-Momentum

FLRW Friedmann-Lemaître-Robertson-Walker

GR General Relativity

HBB Hot Big Bang

KG Klein-Gordon

LHS Left-Hand Side

LSS Last Scattering Surface

RHS Right-Hand Side

SEC Strong Energy Condition

SR Slow-Roll

SRI Slow-Roll Inflation

SSS Static and Spherically Symmetric

CHAPTER 1

BASICS OF COSMOLOGY

Physical Cosmology is a branch of physics which aims at describing the large-scale structure of our Universe, along with its origin, evolution and its ultimate destiny. In this first chapter we are going to give a quick discussion of the *Standard Cosmological Model* which is the basis of Modern Cosmology. Therefore, this lies the foundations for all the discussions we are going to face throughout the following chapters.

1.1. The Principles of Cosmology

Our description of the Universe, and therefore the whole Modern Cosmology, relies on the Standard Cosmological Model, which includes two principles:

1. The Copernican Principle
   This principle states that we are not preferred observers in the Universe.

2. The Cosmological Principle
   The Cosmological Principle asserts that the Universe is homogeneous and isotropic. Obviously, this cannot be true if we stick to small scales, but as long as we observe the Universe at large scales, matter seems to be isotropically distributed on average. Homogeneity is then a consequence of the Copernican Principle, isotropy being independent of the observational point.
   Actually, the Cosmological Principle can be tested: in particular, the transition scale to homogeneity is of order $\sim 100\,\mathrm{Mpc}$ [12]. This result quantifies what we mean with "large scales". On top of this, the isotropy of the Cosmic

Microwave Background (henceforth CMB) is a further key observation which strengthen the Cosmological Principle.

Observations seem to support the Standard Cosmological Model so far. This means that it is a working assumption somehow, in the sense that we assume it, we build our models and eventually we check whether they are consistent with observations or not. In fact, it is the model itself which tells us how signals propagates towards us, and basically these signals are what we turn into observations.
Let us just point out one thing: when we state that the Universe is homogeneous and isotropic we are saying that it is a spacetime solution to Einstein field equations and it is possible to foliate it with 3D spatial hypersurfaces Σ_t such that on each of them we have homogeneity and isotropy.

1.2. The Friedmann-Lemaître-Robertson-Walker spacetime

The Cosmological Principle turns out to be very important because it fixes uniquely the form of our metric: for a homogeneous and isotropic spacetime the metric is given by the well-known Friedmann-Lemaître-Robertson-Walker (FLRW) solution[1]

$$ds^2 = -dt^2 + a^2(t)\left[\frac{dr^2}{1-kr^2} + r^2(d\theta^2 + \sin^2\theta d\phi^2)\right] \tag{1.1}$$

where

- t is the proper time of an observer comoving with the cosmic fluid (which is how we idealise galaxies/clusters on large scales) at r, θ, ϕ constant.
- $a(t)$ is the *scale factor*.
- k is the *curvature constant* which can take three values, i.e. $k = 0, \pm 1$.

According to the value of k, we can have three different scenarios:

1) Flat Universe ($k = 0$)
   In this case, r looks like the usual radial coordinate in $\mathbb{R}^3$: spacelike foliations are 3D Euclidean spaces

$$d\sigma^2 = dr^2 + r^2 d\Omega^2 = dx^2 + dy^2 + dz^2\,.$$

   Hence, the Universe is flat.

[1]We will adopt the mostly plus convention for the metric signature.

2) Closed Universe ($k = 1$)
   If $k = 1$ we set $r = \sin(X)$ and the spatial hypersurfaces are

$$d\sigma^2 = dX^2 + \sin^2(X)d\Omega^2$$

   which are 2-spheres and that is why we say the Universe is closed.

3) Open Universe ($k = -1$)
   In this case, we change coordinates via $r = \sinh(\psi)$ so as to have

$$d\sigma^2 = d\psi^2 + \sinh^2(\psi)d\Omega^2$$

   meaning Σ_t is a hyperboloid and the Universe is open.

1.3. Cosmic fluids

Assuming a FLRW spacetime, homogeneity and isotropy force the energy-momentum (EM) tensor to be

$$T^{\mu}{}_{\nu} = \mathrm{diag}(-\rho, p, p, p) \tag{1.2}$$

where both ρ and p are in general time-dependent (being homogeneously and isotropically distributed). In particular, the energy-momentum tensor obeys the covariant continuity equation

$$\nabla_\mu T^{\mu}{}_{\nu} = 0 \tag{1.3}$$

and if we look at the 00-th component, we find the energy conservation equation given by

$$\dot{\rho} + 3H(\rho + p) = 0 \tag{1.4}$$

where

$$H = \frac{\dot{a}}{a} \tag{1.5}$$

is the *Hubble parameter*.

Now, it is customary to assume an *equation of state*, that is to say a relation between the energy density and the pressure. A well-known choice is the form of a perfect barotropic fluid, namely

$$p = \omega\rho\,. \tag{1.6}$$

This is mainly done for two reasons: first of all, it helps us to cover different physical scenarios; secondly, it enables us to solve equations. For instance, combining Eqs. (1.4) and (1.6) we get

$$\dot{\rho} = -3H\rho(1 + \omega) \tag{1.7}$$

whose solution is given by

$$\rho(t) = \rho_0 \left(\frac{a_0}{a}\right)^{3(1+\omega)} . \tag{1.8}$$

We are used to distinguishing three cases:

1. **Dust**
   In this case, we are dealing with matter with zero pressure. Basically, the only interaction here is provided by gravity.
   Being $p = 0$, the equation of state entails $\omega = 0$ and from Eq. (1.8) we have

   $$\rho_m \propto a^{-3} . \tag{1.9}$$

   For instance, stars, galaxies and clusters can be seen as dust particles comoving with the cosmic fluid, which means they are at fixed values of r, θ and ϕ. On top of this, only gravity has an effect on them, and this implies dust moves along geodesics, since trajectories of constant r, θ, ϕ are geodesics.

2. **Radiation**
   For radiation, the trace of the EM tensor is vanishing, so that $p = \rho/3$, suggesting that $\omega = 1/3$. Therefore

   $$\rho_\gamma \propto a^{-4} . \tag{1.10}$$

3. **Cosmological constant** or **Vacuum energy** or **Dark Energy**
   A third possibility is given by a fluid with the following equation of state:

   $$\rho_\Lambda = -p = \frac{\Lambda}{8\pi G} ,$$

   i.e. $\omega = -1$. We can see how the energy density does not vary with the scale factor, and this is the reason why we call this *vacuum energy.*

1.4. The Friedmann equations

If we consider the FLRW metric and the EM tensor for a perfect fluid, Einstein equations produce the so called *Friedmann equations.* In particular, the 00-th component of the field equations yields

$$3\left[\left(\frac{\dot{a}}{a}\right)^2 + \frac{k}{a^2}\right] = 8\pi G\rho , \tag{1.11}$$

whereas from the ii-th component we get

$$3\frac{\ddot{a}}{a} = -4\pi G(\rho + 3p)\,. \tag{1.12}$$

These equations are not independent: one can show that, starting from the time derivative of Eq. (1.11) and using the conservation law (1.4), we can find again Eq. (1.12).

The Friedmann equation is very important because, provided we are able to solve it, we can find the behaviour of the scale factor. If we consider a matter-dominated (so Eq. (1.9) holds) flat (i.e. $k = 0$) Universe, then Eq. (1.11) yields

$$\frac{\dot{a}^2}{a^2} \sim \frac{1}{a^3} \quad \Leftrightarrow \quad \sqrt{a}\, da \sim dt\,,$$

i.e.

$$a \sim t^{2/3}\,.$$

Similarly, for a radiation-dominated flat Universe one can see that

$$a \sim t^{1/2}\,.$$

Finally, for a flat Universe with only vacuum energy, $\rho_\Lambda \sim \Lambda$ and the Friedmann eq. (1.11) reads

$$\frac{\dot{a}}{a} \sim \sqrt{\frac{\Lambda}{3}} \equiv H_0$$

yielding

$$a \sim e^{H_0 t}\,,$$

which represents a *deSitter Universe* which is exponentially expanding, where H_0 is called *Hubble constant*.

1.5. The expansion of the Universe

Whenever we have a model in our hands, we must try to find a contact with observation. In other words, we shall have some observables in our model which can prove it or not (or actually we had better say that a model can only be falsifiable: this is the principle of falsifiability by the philosopher of science Karl Popper).

1.5.1 The cosmological redshift

Imagine we have a source and a receiver that are comoving with the cosmic fluid. The former is located at $r = r_1$ whereas the latter at $r = r_2$. A first signal is sent from the source at a time t_1 and is received at $t = t_2$. Then, a second signal leaves the source at $t = t_1 + \delta t_1$ reaching the receiver at $t = t_2 + \delta t_2$. They both travel at $\theta, \phi =$ const. so, being for them $ds^2 = 0$, Eq. (1.1) entails

$$\int_{t_1}^{t_2} \frac{dt}{a(t)} = \int_{r_1}^{r_2} \frac{dr}{\sqrt{1-kr^2}} = \int_{t_1+\delta t_1}^{t_2+\delta t_2} \frac{dt}{a(t)} \,.$$

Let us consider the equality between the leftmost and the rightmost side of the previous equation and let us split the integrals as follows:

$$\int_{t_1}^{t_2} = \int_{t_1}^{t_1+\delta t_1} + \int_{t_1+\delta t_1}^{t_2} = \int_{t_1+\delta t_1}^{t_2+\delta t_2} \,.$$

Hence, moving $\int_{t_1+\delta t_1}^{t_2}$ to the right side we have

$$\int_{t_1}^{t_1+\delta t_1} \frac{dt}{a(t)} = \int_{t_2}^{t_2+\delta t_2} \frac{dt}{a(t)} \,.$$

It is reasonable to assume that $\delta t_{1,2}$ are small enough in such a way that $a(t)$ does not change appreciably. This is not strange, if we think of δt as the period of oscillation of the source emitting electromagnetic waves. Therefore, we get

$$\frac{\delta t_1}{a(t_1)} = \frac{\delta t_2}{a(t_2)} \,.$$

Thanks to this equation, we have a connection between δt_1 (the inverse of the frequency of the source as seen by the source itself) and δt_2 (the same as before, but seen by the receiver) which reads[2]

$$\frac{\nu(t_1)}{\nu(t_2)} = \frac{a(t_2)}{a(t_1)} \equiv \frac{a_\mathrm{o}}{a_\mathrm{s}} \,. \tag{1.13}$$

This effect is known as the cosmological redshift. However, for historical reasons, it is usually expressed in terms of wavelengths as

$$z = \frac{\lambda_\mathrm{o} - \lambda_\mathrm{s}}{\lambda_\mathrm{s}} = \frac{a_\mathrm{o}}{a_\mathrm{s}} - 1 \,, \tag{1.14}$$

where the quantity z is called *redshift*. Still, keep in mind that the actual redshift is given by $z + 1$.

It is important to remark that the cosmological redshift is a consequence of the spacetime expansion and it is a measurable quantity.

[2]With the subscripts o and s we refer respectively to the observer/receiver and to the source.

1.5.2 The luminosity-distance relation

The *luminosity-distance relation* provides a way to estimate distances. Let us consider the flux of energy F (i.e. energy per unit time and area) measured by an observer. Let us call $L = E/T$ the luminosity, i.e. the energy per unit time which crosses any concentric sphere. Now, if we imagine our spacetime is Minkowskian, there is no redshift at all, and the luminosity we observe is the same as the one we would measure directly at the source, that we call $L_0 = E_0/T_0$. Then, the flux associated with a sphere of radius R is

$$F = \frac{L}{A} = \frac{L_0}{4\pi R^2} \,.$$

We call $R = d_L$ which is the luminosity-distance; for Minkowski it is clearly given by $d_L^2 = L_0/(4\pi F)$. Obviously, we are not able to measure L_0 so there must be a way to estimate it (see for example the *standard candles*: they are a class of sources whose luminosity is known).

What about if we consider FLRW? Setting the source at $r = 0$, the 2-sphere line element is $a^2 r^2 d\Omega^2$. This means the area of a concentric 2-sphere is given by $4\pi(a_o r)^2$, where a_o is the scale factor at the time of observation. Now, recall that $L = E/T$; therefore, we have to take into account two things: first of all, the energy redshifts like $1/(1+z)$, as a consequence of Eq. (1.13). Then, if we look at T as the time between two discrete emissions, in an expanding Universe they will be detected as two signals separated by a time $(1+z)T$. Thus, $L \simeq L_0/(1+z)^2$, meaning that

$$F = \frac{L}{A} \simeq \frac{L_0}{4\pi(a_o r)^2(1+z)^2} \equiv \frac{L_0}{4\pi d_L^2} \,,$$

that is to say

$$d_L = a_o r(1+z) \,.$$

1.5.3 The Hubble law

The Hubble law is an important result since it shows that the Universe is expanding. It connects the distance and the redshift z through an (almost) linear relation.

In order to see where it comes from, let us consider a radial photon in a FLRW spacetime. We have seen it redshifts according to Eq. (1.14), which we rewrite as

$$z(t_s) = \frac{a_o}{a(t_s)} - 1 \,.$$

For not so distant objects, the photon does not take too much time to reach us, i.e. the quantity $(t_o - t_s)$ is small. Therefore, we can expand $a(t_s)$ around t_o as

$a(t_s) = a_o + \dot{a}_o(t_s - t_o) + ...$, so that

$$z(t_s) = \frac{a_o}{a_o}\left[1 + H_o(t_s - t_o) + ...\right]^{-1} - 1 \simeq H_o(t_o - t_s)\,.$$

Since we are considering a radial photon, we have $dt^2 = dr^2$ which means the travel time is equal to the distance to the emitter, i.e. $t_o - t_s = r$. We then get the Hubble law:

$$z = H_o r \tag{1.15}$$

which holds for $z \ll 1$. The further we go, the larger the redshift is, meaning that distant galaxies are receding faster with respect to closer ones.

CHAPTER 2

INFLATIONARY COSMOLOGY

Nowadays, the most widely adopted cosmological model for the description of the evolution of our Universe is the so called *Hot Big Bang theory* (HBB). Its validity is backed by many experimental data, such as the abundances of light elements according to Big Bang Nucleosynthesis (BBN), the CMB (see Appendix A) and so on. Yet, we shall draw our attention to the fact that, quoting Jim Peebles's[1] words, such a model is describing "how our Universe is evolving, not how it began". The point is that the HBB model suffers for several problems. One of the possible proposals to fix this is the *Inflationary theory*: basically, during inflation the Universe underwent an extremely rapid expansion in such a way its size increased enormously. It is able to solve many of the problems afflicting the HBB theory in an elegant way.
The purpose of this chapter is to give a brief introduction to some of the HBB drawbacks and describe the inflationary theory thereafter.

2.1. The horizon problem

We have said that our Universe is highly homogeneous and isotropic on large scales. The best measure of this fact is provided by the CMB temperature anisotropy: the average value of the CMB temperature today is given by (see [7])

$$T_0 = 2.7260 \pm 0.0013\,\mathrm{K}\,. \tag{2.1}$$

[1]2019 Nobel Prize in Physics.

The CMB anisotropy is of the order

$$\frac{\delta T}{T_0} \simeq 10^{-4} \div 10^{-5}$$

which is very small with respect to T_0. The point is that this scenario seems to be extremely unlikely: in fact, within the HBB model, the sky is made up of a large number of causally disconnected patches, as we are going to see in a while. Therefore, this clashes with the degree of homogeneity of the CMB. This issue is what is called *horizon problem.*

To begin with, we aim to investigate the causal structure of the spacetime so as to understand how different and causally disconnected parts of the sky are at the same temperature without any exchange of information. To this end, we consider a radial ($d\Omega^2 = 0$) photon ($ds^2 = 0$) propagating in a flat FLRW spacetime. Furthermore, we exploit the definition of the *conformal time* τ given by

$$dt = a\, d\tau\,. \tag{2.2}$$

Thus, the FLRW line element looks like

$$dr = d\tau$$

whose integration yields

$$\Delta r = \Delta \tau = \int_{t_i}^{t} \frac{dt'}{a(t')}\,. \tag{2.3}$$

This is the definition of the radial maximal distance a photon can travel between t_i and $t > t_i$. Now, within the HBB, the Big Bang corresponds to $t_i = 0$ with $a(t_i) = 0$, and this let us define the *Comoving particle horizon* as [2]

$$\Delta r_{\max}(t) = \int_{0}^{t} \frac{dt'}{a(t')} = \tau(t) - \tau(0)\,. \tag{2.4}$$

Using both (1.8) and the Friedmann eq. (1.11) with $k = 0$ one can get

$$a^{\frac{3}{2}(1+\omega)} \propto t \tag{2.5}$$

which turns Eq. (2.4) into

$$\Delta r_{\max} \propto a^{\frac{1}{2}(1+\omega)}\,. \tag{2.6}$$

[2] Note the presence of a singularity (physical quantities diverge for a radiation dominated Universe, such as ρ, if $t \to 0$). Usually the starting time is taken to be the Plank time t_p necessary to avoid quantum effects of gravity.

This result shows how the comoving particle horizon is actually finite; as a consequence, in the HBB there were regions that were not in causal contact in the past. In spite of this, they are measured to have the same temperature with a precision of $10^{-4} \div 10^{-5}$. However, it is not strange to find this: even in Minkowski we would get a finite result. Most importantly, we have the explicit dependence of the comoving particle horizon on the scale factor from Eq. (2.6).
We could deal with the horizon issue in a more quantitative way by considering Figure 2.1: we want to compute $d_{\rm hor}$ and d_A in order to have an idea of the angular scale $\theta_{\rm hor}$ of the comoving horizon at recombination.

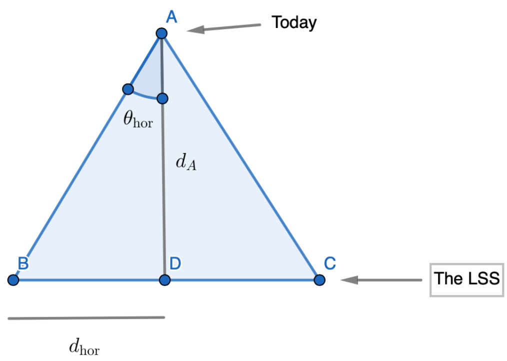

Figure 2.1

For $\theta_{\rm hor}$ small, we have

$$\theta_{\rm hor} \simeq \frac{d_{\rm hor}}{d_A} = \frac{\tau_{\rm rec} - \tau_i}{\tau_o - \tau_{\rm rec}}$$

where $\tau_{\rm rec}$ refers to recombination, $\tau_i = 0$ to the Big Bang and τ_o to today. The computation of both the numerator and denominator proceeds via Eq. (2.3); avoiding some mathematical details, a numerical estimate of those integral yields

$$\theta_{\rm hor} \simeq 1.16^\circ \,.$$

Considering that the points B and C in Figure 2.1 are not in causal contact, we can say that any couple of points on the LSS separated by $\theta > \theta_c \equiv 2\theta_{\rm hor} \simeq 2.3^\circ \simeq 0.04\,\text{rad}$ was never in causal contact. Since the LSS corresponds to a solid angle of 4π, it is made up of approximately $4\pi/(0.04)^2 \sim 10^4$ causally disconnected patches which, however, are at the same temperature. So, to rephrase the horizon problem, how is this possible considering that there was not enough time, between the initial singularity and recombination, to exchange information?

2.2. The flatness problem

The *flatness problem* deals with the extremely high tuned initial conditions that would be required in order to observe the current curvature of the Universe from experiments.
More specifically, from observations we find the following bound:

$$\Omega - 1 < 0.02 \qquad \text{today}, \tag{2.7}$$

where Ω is basically the density of matter and energy and will be defined in a moment. It sounds good to start from this and go backward in time so as to check the required initial conditions that have led to Eq.(2.7).
First of all, the Friedmann eq. (1.11) can be written as

$$H^2 = \frac{8\pi G}{3} \sum_i \rho_i - \frac{k}{a^2}\,. \tag{2.8}$$

Then, we define the i-th density parameter as

$$\Omega_i \equiv \frac{8\pi G}{3H^2} \rho_i = \frac{\rho_i}{\rho_c}$$

where $\rho_c \equiv 3H^2/(8\pi G)$ is the *critical density.* The total density parameter is

$$\Omega \equiv \sum_i \Omega_i$$

and Eq. (2.8) reads

$$\Omega - 1 = \frac{k}{(aH)^2}\,. \tag{2.9}$$

We now compare Eq. (2.9) between today and the Planck time, keeping in mind the bound (2.7):

$$\frac{\Omega(t_o) - 1}{\Omega(t_P) - 1} = \frac{(aH)^2|_{t_P}}{(aH)^2|_{t_o}} = \left(\frac{a(t_P)}{a(t_o)}\right)^2 \left(\frac{H(t_P)}{H(t_o)}\right)^2 , \tag{2.10}$$

where t_o refers to today and t_P is the Planck time. We then exploit the following relations:

$$\begin{aligned} H(t_P) &\sim M_P \\ T_P &\sim M_P \\ a(T) &\sim \frac{1}{T} \qquad \text{for a gas of photons}\,, \end{aligned}$$

where now T_P is the Planck temperature, T is a generic temperature and M_P is the Planck Mass, defined as $M_P^2 = (8\pi G)^{-1}$. Then, Eq. (2.10) becomes

$$\frac{\Omega(t_o)-1}{\Omega(t_P)-1} = \left(\frac{T_o}{M_P}\right)^2 \left(\frac{M_P}{Ho}\right)^2 = \left(\frac{T_o}{H_o}\right)^2 .$$

Experimental data provide us with $T_o \simeq 2.7\,\mathrm{K}$ and $H_o \simeq 10^{-60} M_P$, which means

$$\frac{\Omega(t_o)-1}{\Omega(t_P)-1} \simeq 10^{58} .$$

Taking Eq. (2.7) into account, we need to tune

$$\Omega(t_P) - 1 \leq 10^{-60} , \tag{2.11}$$

which is an extreme fine tuning.

2.3. The shrinking comoving Hubble radius: a possible way out

If we look carefully at the treatment we have just done, we can already guess that a possible way out of these problems has to do with the factor $(aH)^{-1}$, which is called *comoving Hubble radius* (CHR). In fact, it appears in Eq. (2.4) if we write it as

$$\tau = \int d\ln(a)(aH)^{-1} , \tag{2.12}$$

and also in Eq. (2.9). In particular, Eq. (2.12) shows how the elapsed conformal time is connected to the evolution of the CHR. We are going to see that a given behaviour of the CHR is able to solve our previous problems.
To begin with, one can invert Eq. (2.5) and ultimately find that

$$(aH)^{-1} \propto a^{\frac{1}{2}(1+3\omega)} . \tag{2.13}$$

Familiar energy sources satisfy the strong energy condition (SEC), which reads $1 + 3\omega > 0$. Thus, Eq. (2.13) entails that, for SEC-obeying sources, the CHR increases as the Universe expands, or in other terms

$$\frac{d(aH)^{-1}}{dt} > 0 \quad \text{if SEC is satisfied} .$$

Now, if we solve the integral in Eq. (2.12) using Eq. (2.13), we get

$$\tau \propto \frac{2}{1+3\omega} a^{\frac{1+3\omega}{2}} . \tag{2.14}$$

The initial singularity $a(\tau_i) = 0$ within the HBB model is located at $\tau_i = 0$, and $\tau \in [0, +\infty)$ when the SEC holds. However, things change dramatically if we allow for a SEC-violating source. In this case, $\omega < -1/3$ and consequently the CHR decreases as the Universe expands. Moreover, Eq. (2.14) implies that the initial singularity $a = 0$ is dragged back to $\tau_i = -\infty$. Let us check how this solves both the horizon and the flatness problems.

2.3.1 Solution to the horizon problem

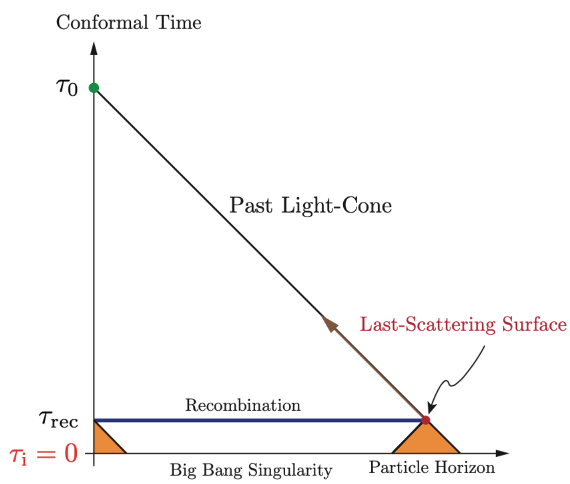

Figure 2.2: Structure of the CMB light cones for a standard FLRW cosmology. τ_0 refers to today.
© Copyright [1].

First of all, let us focus on the horizon problem. From Fig. 2.2 we can clearly see how different patches on the LSS were not in causal contact. Nevertheless, if we let $\tau_i \to -\infty$ via a SEC-violating matter source, then we get what is shown in Fig. 2.3: basically, the amount of elapsed conformal time between the initial singularity and recombination is increased. This makes sure that points of the CMB that were not in causal contact according to our previous treatment have now overlapping past light cones. In this scenario, $\tau = 0$ correspond to the end of inflation, which is also known as *reheating*.[3] Inflation would therefore be a period of the evolution of our Universe where the latter was dominated by a matter source which violated the

[3] The reheating is the transition period where the inflationary media is supposed to be converted into ordinary matter.

SEC. In this respect, it is important to point out that we know the condition to solve the problem (i.e. a decreasing CHR or SEC-violating source, equivalently), but we still need to find what kind of matter gives this result.

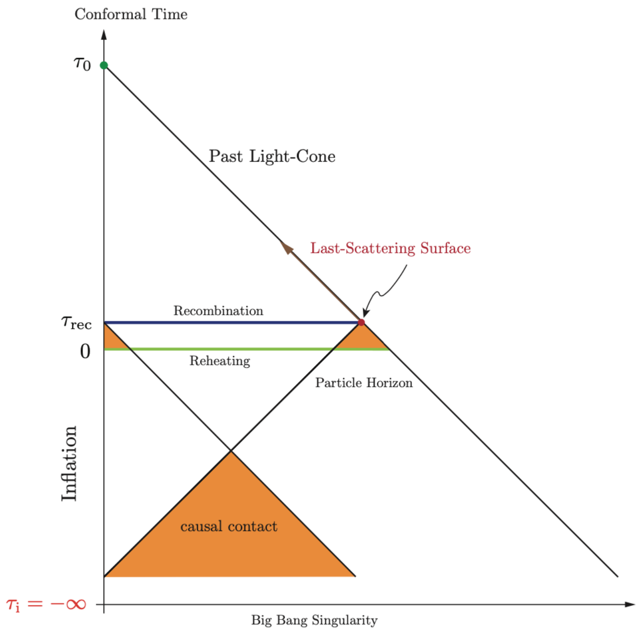

Figure 2.3: Structure of the CMB light cones for inflationary cosmology.
© Copyright [1].

2.3.2 Solution to the flatness problem

Moving to the flatness problem, we had seen how we needed an extreme tuning at early times (see Eq. (2.11)) in order to explain what we observe today concerning $\Omega - 1$. However, let us focus on Eq. (2.9): it is manifest that $\Omega - 1$ evolves according to the square of the CHR. As a consequence, when we consider a SEC-obeying source, $(aH)^{-1}$ increases with the expansion of the Universe, letting $\Omega - 1$ grow. On the other hand, when we take inflation into account $(aH)^{-1}$ decreases and $\Omega = 1$ is what is called an attractor during inflation. In this way, a decreasing CHR solves the flatness problem, as well.

2.3.3 Equivalent conditions for inflation

We have just seen which conditions enable us to solve dinamically the problems related to the HBB model. However, those conditions can be recast in a different fashion; in other words, we are going to list different but equivalent conditions for inflation:

1) Decreasing CHR

2) SEC violating source

3) Matter source with negative pressure
This follows immediately from the requirement that SEC must be violated and from the equation of state (1.6), upon requiring $\rho > 0$.

4) Accelerated expansion of the Universe
Let us consider the flat Friedmann eq. (set now for simplicity $8\pi G = 1$)

$$H^2 = \frac{\rho}{3},$$

which can be written as

$$\dot{a} = \sqrt{\frac{\rho}{3}}a\,. \tag{2.15}$$

Let us take the time derivative in order to get the acceleration related to the scale factor:

$$\ddot{a} = \dot{a}\sqrt{\frac{\rho}{3}} + \frac{a\dot{\rho}}{2\sqrt{3\rho}} = \frac{\rho}{3}a - \frac{a}{2\sqrt{3\rho}}3H\rho(1+\omega)\,,$$

where in the last equality we have employed Eqs. (2.15) and (1.7). Writing $H = \sqrt{\rho/3}$ we get

$$\ddot{a} = \frac{\rho}{3}a - \frac{a}{2}\rho(1+\omega) = -\frac{\rho a}{6}(1+3\omega)\,. \tag{2.16}$$

Then, the condition $\omega < -1/3$ clearly results into $\ddot{a} > 0$.

5) Slowly varying Hubble parameter
Starting from the definition of H we can easily get

$$\frac{\dot{H}}{H^2} = \frac{\ddot{a}a}{\dot{a}^2} - 1\,.$$

By means of Eqs. (2.15) and (2.16) we have

$$\frac{\dot{H}}{H^2} = -\frac{3}{2}(1+\omega)\,.$$

Let us define the *first slow roll parameter* (or *Hubble slow roll parameter*; we are going to come back on this in a moment when we discuss slow roll inflation) as

$$\epsilon_{\mathrm{H}} \equiv -\frac{\dot{H}}{H^2} = \frac{3}{2}(1+\omega)\,. \tag{2.17}$$

The SEC-violating condition enforces $\epsilon_{\mathrm{H}} < 1$, which means the Hubble parameter H has to vary slowly.

2.3.4 Duration of inflation: a minimum estimate

We can give a rough estimate about the duration of inflation. To this end, let us introduce a quantity called *number of e-foldings*, given by

$$N \equiv \ln(a)\,. \tag{2.18}$$

It is adopted as a time variable and it turns out to be useful, especially during inflation. In general, an e-folding is the amount of time required by an exponentially-growing quantity to increase by a factor of e. In fact, the definition (2.18) shows how, in N_e e-folds, the Universe expanded by a factor e^{N_e}.

Now, in order to have an idea of the duration of inflation, let us go back to the treatment of the flatness problem and recast Eq. (2.10) as follows:

$$\frac{\Omega(t)-1}{\Omega(t_o)-1} = \left(\frac{a_o H_o}{a(t)H(t)}\right)^2 ,$$

with t_o and t corresponding to the present time and the start of inflation respectively. It is reasonable to expect that the quantity $\Omega(t) - 1 \equiv \Omega_{\text{curv}}(t) \sim o(1)$ so that the bound (2.7) ensures the LHS of the previous equation is a large number, that is to say

$$\left(\frac{a_o H_o}{a(t)H(t)}\right)^2 \gg 1\,.$$

Next, we introduce a_{end} and H_{end} as the scale factor and the Hubble parameter evaluated at the end of inflation and we manipulate the previous result:

$$\left(\frac{a_o}{a_{\text{end}}}\right)^2 \left(\frac{a_{\text{end}}}{a(t)}\right)^2 \left(\frac{H_o}{H_{\text{end}}}\right)^2 \left(\frac{H_{\text{end}}}{H(t)}\right)^2 \gg 1\,.$$

During inflation, the Hubble parameter varies very slowly; hence, it comes natural to assume $H_{\text{end}} \sim H(t)$ and take the logarithm of the previous inequality to get

$$\ln\left(\frac{a_o}{a_{\text{end}}}\right) + \ln\left(\frac{a_{\text{end}}}{a(t)}\right) + \ln\left(\frac{H_o}{H_{\text{end}}}\right) \gg 0\,.$$

Now, during inflation the Universe expanded by a factor $\frac{a_{\text{end}}}{a(t)} = e^{N_{\text{tot}}}$, where N_{tot} is the total number of e-folds associated with inflation, so it is exactly what we would like to estimate. To do so, we consider that $\rho_{\text{rad}} \sim a^{-4} \sim T^4$, i.e. $a \sim 1/T$, so that [4]

$$a_{\text{end}} \sim \frac{1}{T_{reh}} \qquad\qquad a_o \sim \frac{1}{T_o}\,,$$

[4]Recall that the end of inflation is also called reheating.

where $T_o \simeq 2.73\,\mathrm{K}$. With this at hand, we get

$$N_{\text{tot}} > \ln\left(\frac{H_{\text{end}}}{T_{\text{reh}}}\right) + \ln\left(\frac{T_o}{H_o}\right) .$$

Recalling $H_o \simeq 10^{-60} M_P$ and $H_{\text{end}} \sim H_{\text{inf}}$ we find

$$N_{\text{tot}} \gtrsim 66 + \ln\left(\frac{H_{\text{inf}}}{T_{\text{reh}}}\right) = N_{\text{tot}}^{(\text{min})} . \tag{2.19}$$

The second term sitting the RHS in Eq. (2.19) is model-dependent, but eventually the range is $N_{\text{tot}}^{(\text{min})} \simeq 70 \div 100$. Anyway, more accurate discussions let us safely assume $N_{\text{tot}}^{\text{min}} \simeq 60$ for a standard inflationary model, even though for particular models one has to be more careful (see, for instance, [14]).
A further step would produce an estimate of the time elapsed between the beginning and the end of inflation. We have seen that the total number of e-folds during inflation is $N_{\text{tot}} = \ln(a_{\text{end}}/a(t))$, which can be written as

$$N_{\text{tot}} = \int_{a(t)}^{a_{\text{end}}} d\ln(a) = \int_{t}^{t_{\text{end}}} H(t)dt .$$

Assuming, as usual, a constant Hubble parameter during inflation, we can write the following approximation:

$$N_{\text{tot}} \simeq H_{\text{inf}} \int_{t}^{t_{\text{end}}} dt = H_{\text{inf}} \Delta t_{\text{inf}} .$$

According to the model, one eventually has

$$\Delta t_{\text{inf}}^{(\text{min})} \simeq 10^{-42} \div 10^{-9} s \tag{2.20}$$

which is a clear signal of an extraordinary rapid event during which the scale factor became something like 10^{25} times larger than it was when inflation began.[5] Thus, the volume of the Universe grew of a factor which is approximately given by $(10^{25})^3 = 10^{75}$.

2.4. Slow-roll inflation

So far we have seen a way to overcome the problems associated with the HBB model, and we have called it inflation. However, note that we have actually pointed out inflation has to happen, how long it has to last, but we have not explained how it has to occur yet. In other words, we still have to answer the following question: "What

[5]Here, again, we are assuming 60 e-foldings.

kind of matter do we need in order to generate such an accelerated expansion of the Universe?".

At first glance, we might take into consideration the model represented by the cosmological constant. It is indeed a toy model satisfying the condition for inflation, being $\omega = -1$ for instance. In addition, we have also described how it is related to a dS Universe which is exponentially expanding. Still, if we think about it carefully, the dS Universe is empty and eternal. This clashes with inflation, since we want it to last for a very tiny (and therefore finite) amount of time. Moreover, when we say empty it means there is no other form of matter embedded inside the EM tensor and this is in contradiction with current observations. In short, a dS Universe is not a good model for inflation.

The model we are going to present is known as *slow roll inflation*. We consider the usual Einstein-Hilbert action and a minimally coupled scalar field ϕ called the *inflaton* (by the way, we assume a homogeneous inflaton, $\phi = \phi(t)$), namely

$$\mathcal{S} = \int d^4x\sqrt{-g}\left[\frac{M_P^2}{2}R - \frac{1}{2}g^{\mu\nu}\partial_\mu\phi\partial_\nu\phi - V(\phi)\right], \tag{2.21}$$

where R is the Ricci scalar and $-g$ is the absolute value of the determinant of the metric $g^{\mu\nu}$; $V(\phi)$ is still an arbitrary function. This is the minimum set-up so as to get SRI. The general expression for the EM tensor in GR is given by

$$T_{\mu\nu} = \frac{-2}{\sqrt{-g}}\frac{\delta S_M}{\delta g^{\mu\nu}} = -2\frac{\partial\mathcal{L}_M}{\partial g^{\mu\nu}} + g_{\mu\nu}\mathcal{L}_M\,, \tag{2.22}$$

where the subscript M refers to the matter part of the action/Lagrangian. Hence, for the action (2.21) we get

$$T_{\mu\nu} = \partial_\mu\phi\partial_\nu\phi + g_{\mu\nu}\mathcal{L}_M\,. \tag{2.23}$$

We assume a flat FLRW background metric and, recalling that the inflaton depends only on t, it is easy to check that Eq. (2.23) yields

$$T_{00} = \rho = \frac{\dot{\phi}^2}{2} + V(\phi)\,, \tag{2.24}$$

$$T_{ii} = a^2\left(\frac{\dot{\phi}^2}{2} - V(\phi)\right) = a^2 p\,. \tag{2.25}$$

The time evolution of the inflaton can be obtained from the action and is given by the following Klein-Gordon (KG) equation

$$\ddot{\phi} + 3H\dot{\phi} = -\partial_\phi V\,. \tag{2.26}$$

The Friedmann eq. is straightforward from Eq. (2.24)

$$H^2 = \frac{\rho}{3M_P^2} = \frac{1}{3M_P^2}\left(\frac{\dot{\phi}^2}{2} + V\right) . \tag{2.27}$$

Let us now consider the eq. of state (1.6):

$$\omega = \frac{p}{\rho} = \frac{\frac{\dot{\phi}^2}{2} - V}{\frac{\dot{\phi}^2}{2} + V} . \tag{2.28}$$

The idea behind SRI is to have a sort of deformation of a dS Universe, i.e. something very close to a cosmological constant which has a finite extension in time. Hence, requiring $\omega \simeq -1$ implies from Eq. (2.28) $\frac{\dot{\phi}^2}{2} \ll V$. This condition reflects on the first SR parameter defined in Eq. (2.17) as

$$\epsilon_{\rm H} \ll 1 \tag{2.29}$$

which is called *slow roll condition*. It has to be true as long as inflation is operating. The inequality $\dot{\phi}^2/2 \ll V$ is the reason why we call such a model SRI: the scalar field is slowly rolling down its potential and the dominant contribution to the energy/pressure is given by the potential rather than the kinetic energy.
We now define the *second slow roll parameter* $\eta_{\rm H}$, which keeps track of the variation of $\epsilon_{\rm H}$:

$$\eta_{\rm H} \equiv \frac{d\ln(\epsilon_{\rm H})}{dN} = \frac{\dot{\epsilon}_{\rm H}}{H\epsilon_{\rm H}} , \tag{2.30}$$

where the straightforward relation

$$\frac{d}{dt} = H\frac{d}{dN} \tag{2.31}$$

has been employed. We require $\eta_{\rm H} \ll 1$ (*second slow roll condition*) in order for inflation to keep going. Let us clarify this: the first SR condition makes sure $\omega \simeq -1$ holds, and from the equation of state we have a constant energy density like a cosmological constant, so that we have an exponential expansion. Then, in order to make inflation long enough, the second SR condition ensures that we stay for a sufficient amount of time in the phase defined by the first SR condition. We could go on and define a third SR parameter, but it is sufficient to stop here and just point out the fact that when the SR parameters are no longer small, inflation ends.
Let us recast the SR conditions $\epsilon_{\rm H}, \eta_{\rm H} \ll 1$ as conditions on the potential $V(\phi)$. We

define the so called *potential slow roll parameters* as

$$\epsilon_{\mathrm{V}} \equiv \frac{M_P^2}{2}\left(\frac{\partial_\phi V}{V}\right)^2 , \tag{2.32}$$

$$\eta_{\mathrm{V}} \equiv M_P^2 \frac{\partial_{\phi\phi} V}{V} . \tag{2.33}$$

One can show that

$$\epsilon_{\mathrm{H}} = \epsilon_{\mathrm{V}} , \tag{2.34}$$

$$\eta_{\mathrm{H}} = -2\eta_{\mathrm{V}} + 4\epsilon_{\mathrm{V}} . \tag{2.35}$$

Therefore, the SR conditions become

$$\frac{\partial_\phi V}{V} \ll 1 \qquad \frac{\partial_{\phi\phi} V}{V} \ll 1 , \tag{2.36}$$

i.e. an almost flat potential during inflation.
Let us conclude this discussion with a recap/better clarification of the idea at the basis of SRI: we have a quasi dS Universe, i.e. a deformed dS Universe where we introduce a scalar field (the scalar field is the easiest option). Why do we act like this? The introduction of a homogeneous field whose energy density is constant during inflation (we have seen it is dominated by a quasi flat potential) ensures we have an exponential expansion. Yet, this expansion must end at some point of the history of the Universe: in order to put an end to inflation, some mechanism must occur, and this is what we call reheating. Forget about the machinery behind reheating (this goes far beyond our purposes), the scalar field somehow disappears generating ordinary matter. The presence of the cosmological constant, associated with a constant vacuum energy, enables the exponential expansion to work at late time as well, whereas the energy density of matter in the Universe decreases as it is expanding.

CHAPTER 3

SCALAR FIELD COSMOLOGY WITH AN EXPONENTIAL POTENTIAL

In the previous chapter we have introduced the inflationary theory; in particular, we have discussed SRI, which is based on the action (2.21). However, we have not seen any specific model, being $V(\phi)$ arbitrary so far.
In this chapter we would like to study a given cosmology whose potential takes an exponential form as follows

$$V(\phi) = V_0\, e^{-\lambda \frac{\phi}{M_P}} \,, \tag{3.1}$$

where $M_P^2 = (8\pi\, G)^{-1}$ is the gravitational coupling and λ is a dimensionless constant associated with the slope of the potential. Let us stress that, a priori, we are not dealing with an inflationary model. Exponential potentials have been adopted for the study of various situations, such as period of early inflation, but also for the ekpyrotic Universe or pre Big Bang collapse.[1]
Our goal here is to study the dynamics of such a cosmology in the phase-space using a system of dimensionless dynamical variables. We will investigate the different scenarios related to the sign of the potential, which can be either positive or negative. To conclude this chapter, we discuss a so called "cosmic no-hair theorem" for contracting universes so as to show that contracting cosmologies are important not only for a FLRW spacetime.

[1]The ekpyrotic scenario describes a slowly contracting Universe with a subsequent bounce.

3.1. Dynamical equations

We consider the following matter Lagrangian for our scalar field

$$\mathcal{L}_M = -\frac{1}{2}\partial_\mu\phi\partial^\mu\phi - V(\phi) \tag{3.2}$$

with $V(\phi)$ as in Eq. (3.1). We leave the sign of the potential implicitly arbitrary by means of V_0 (the standard case is $V_0 > 0$). We will face the cases $\pm V > 0$ later on. Our background is given by a flat FLRW Universe, so that the KG equation for our scalar field and the Hubble parameter are provided by Eqs. (2.26) and (2.27) respectively. As anticipated before, we consider the following set of dimensionless variables

$$x \equiv \frac{\dot{\phi}}{M_P\sqrt{6}H}\,, \tag{3.3}$$

$$y \equiv \frac{\sqrt{|V|}}{M_P\sqrt{3}H} \tag{3.4}$$

which enable us to write down the Friedmann equation (2.27) as

$$x^2 \pm y^2 = 1\,. \tag{3.5}$$

Basically, x^2 measures the contribution of the kinetic energy density of our scalar field to the expansion; on the other hand, $\pm y^2$ embodies the contribution of the potential energy density. The $\pm$ sign in front of y^2 accounts for the possibility for V of being respectively positive or negative (i.e. $\pm V > 0$).

With these dimensionless variables, we are able to write down the dynamical equation as an autonomous system (see Appendix B.1)

$$x' = -3x(1-x^2) \pm \lambda\sqrt{\frac{3}{2}}y^2\,, \tag{3.6}$$

$$y' = xy\left(3x - \lambda\sqrt{\frac{3}{2}}\right)\,. \tag{3.7}$$

The prime refers to the derivative with respect to the number of e-foldings. This system is actually connected to a one-dimensional phase-space because of the constraint (3.5). This is what we are going to study in the following section.

Without loss of generality, we can consider $\lambda \geq 0$, since the system is symmetric under $\lambda \to -\lambda$ and $x \to -x$.

3.2. One-dimensional phase-space

We have just seen how the introduction of the dimensionless variables x and y let us write down the dynamical equation as an autonomous system which is associated with a one-dimensional phase-space. The latter corresponds to a unit circle when $V \geq 0$ and to a hyperbola when $V \leq 0$ (see the constraint (3.5)). Now our goal is to discuss (following [13]) the critical points of this system and their stability. In particular, we stick to the part of the phase-plane associated with $y \geq 0$: this corresponds to expanding cosmologies with $H > 0$, but trajectories are actually symmetrical under time reversal, i.e. $H \to -H$ (which is the reflection symmetry $x \to x$, $y \to -y$). In other words, early time expanding solutions look the same as late time collapsing ones.

3.2.1 Critical points and stability

Critical points (x_i, y_i) of a dynamical system are defined as those such that both x' and y' are vanishing. If we consider the differential equation (B.2) and we solve it for the scale factor, for all the critical points such that x_i is a non-vanishing constant we have

$$a(t) \propto |t|^p, \qquad p = \frac{1}{3x_i^2},$$

that is a power-law solution. With this at hand, we go on and consider the possible fixed points of our autonomous system. It admits at most three fixed points:

- Kinetic-dominated solutions

  No matter the form of the potential, the points

  $$A_+ = (1, 0) \qquad A_- = (-1, 0)$$

  are critical points and correspond to the so called *kinetic-dominated solutions*, since the actual contribution is given by $x_{A_\pm} = \pm 1$. In this case, the scale factor evolves like $a \propto t^{1/3}$.

  The study of the stability starts from linear perturbations about the critical points, i.e. $x_i \to x_i + \delta x_i$ and $y_i \to y_i + \delta y_i$. By substituting this into the autonomous system and exploiting the Friedmann constraint (3.5), one can get the system of differential equation for the perturbations δx_i and δy_i. To first order in the perturbations, one has

  $$\begin{pmatrix} \delta x_i' \\ \delta y_i' \end{pmatrix} = \mathbf{A} \begin{pmatrix} \delta x_i \\ \delta y_i \end{pmatrix}.$$

  Ultimately one can find the evolution of the perturbations, which are strictly

connected to the eigenvalues m_j of the matrix $\mathbf{A}$.
For the case at hand, one can check that perturbations evolve as $\delta x_i \propto e^{m_\pm N}$, where $m_+ = \sqrt{6}(\sqrt{6}-\lambda)$ is associated with x_{A_+} and $m_- = \sqrt{6}(\sqrt{6}+\lambda)$ is related to x_{A_-}. Since stability requires the real part of the eigenvalues to be negative, we can conclude that the point A_- is always unstable, while A_+ is stable for $\lambda^2 > 6$ but unstable for $\lambda^2 < 6$.

- Potential-kinetic-scaling solution
A second possible solution is provided by the point

$$B = \left(\frac{\lambda}{\sqrt{6}}, \sqrt{\pm\left(1 - \frac{\lambda^2}{6}\right)} \right) .$$

It is the so called *potential-kinetic-scaling solution*, where the kinetic contribution and the potential contribution are similar. This solution is allowed only when $\pm(6-\lambda^2) > 0$, $\lambda^2 < 6$ corresponding to positive and sufficiently flat potentials and $\lambda^2 > 6$ to negative steep potentials.[2] The exponent $p = 2/\lambda^2$ depends on whether we are dealing with the former or the latter: $p > 1$, i.e. $\lambda^2 < 2$ (and $H > 0$) corresponds to power-law inflation solutions, whereas $p \ll 1$, i.e. $\lambda \gg 1$ (and $H < 0$) is associated to an accelerated collapse.
As far as stability is concerned, linear perturbations evolve according to the eigenvalue $m = (\lambda^2 - 6)/2$; hence, for a positive flat potential we always have stability, but it is unstable if we consider a negative potential.

3.2.2 Qualitative evolution in the phase-space

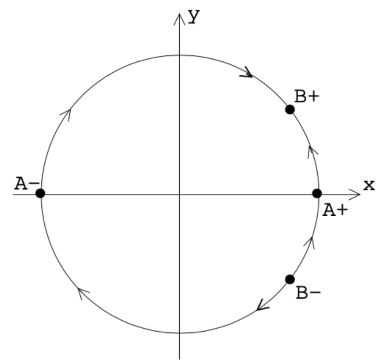

Figure 3.1: 1D phase-space for flat positive potentials. Arrows indicate the evolution with respect to cosmic time t. In the lower part of the plane, where $H < 0$, this has the opposite sense to the number of e-folds N.
© Copyright [13].

[2]Remember that the upper sign is for $V > 0$ whereas the lower sign is for $V < 0$.

At this stage we are able to discuss what happens in the phase-space according to the features of the potential.

1. <u>Flat positive potentials ($V > 0, \quad \lambda^2 < 6$)</u>
   We know that for flat positive potentials all critical points are allowed; in particular, B is a stable late time attractor whereas A_+ and A_- are unstable repellors. As shown in Fig. 3.1, generic solutions starts in a kinetic-dominated regime, approaching the kinetic-potential-scaling solution B at late times. Different physical scenarios are collected in Fig. 3.5.

2. <u>Steep positive potentials ($V > 0, \quad \lambda^2 > 6$)</u>
   In this case, solution B does not exist, and we can consider only A_+ and A_-

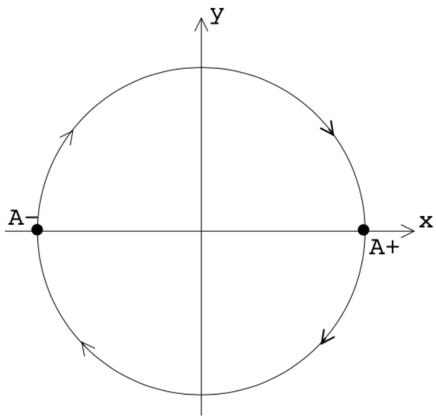

Figure 3.2: 1D phase-space for steep positive potentials.

   which are respectively stable and unstable. Hence, as we can see from Fig. 3.2, generic solutions live in a kinetic-dominated regime, starting from A_- and evolving to A_+ at late times. Just to give the whole picture, in the upper half plane we start from a Big Bang in A_- and we expand towards future infinity represented by A_+. On the other hand, if one looks at it in the lower plane, where the sense of N is opposite, we start from past infinity A_+ and collapse towards a Big Crunch in A_-.

3. <u>Flat negative potentials ($V < 0, \quad \lambda^2 < 6$)</u>
   Also here, solution B is not present. $A_\pm$ are instead both unstable repellors. We see from Fig. 3.3 that we start from one of the kinetic-dominated solution and we go out to infinity, but we recollapse to the other kinetic-dominated solution. This is connected to the fact that, when H changes sign, x and y change sign as well. Therefore, trajectories which exit top-right in Figures 3.3 and 3.4 are connected to those entering bottom-left, and similarly top-left are

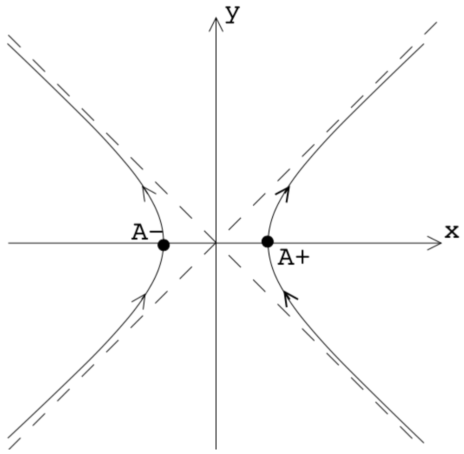

Figure 3.3: 1D phase-space for flat negative potentials.
© Copyright [13].

connected to bottom-right. Just to have a physical grasp, we start from a Big Bang in $A_{\pm}$, the Universe expands and then recollapses to a Big Crunch in $A_{\mp}$.

4. Steep negative potentials ($V < 0, \quad \lambda^2 > 6$)
   Here all the three critical points come into play, but only A_+ is a stable late-

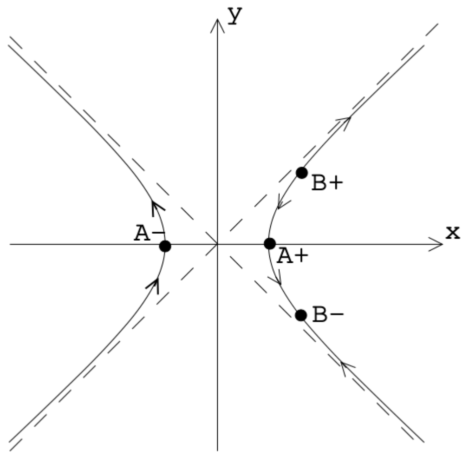

Figure 3.4: 1D phase-space for steep negative potentials.
© Copyright [13].

time attractor. This fact is responsible for the various scenarios that can take place, which have been listed in Fig. 3.5.

Potential		Evolution		
Positive	flat	A_- big bang	$\rightarrow$ expansion	B_+ future infinity
		A_+ big bang	$\rightarrow$ expansion	B_+ future infinity
		B_- past infinity	$\rightarrow$ collapse	A_- big crunch
		B_- past infinity	$\rightarrow$ collapse	A_+ big crunch
	steep	A_- big bang	$\rightarrow$ expansion	A_+ future infinity
		A_+ past infinity	$\rightarrow$ collapse	A_- big crunch
Negative	flat	A_- big bang	$\rightarrow$ expansion and recollapse	A_+ big crunch
		A_+ big bang	$\rightarrow$ expansion and recollapse	A_- big crunch
	steep	B_+ big bang	$\rightarrow$ expansion	A_+ future infinity
		B_+ big bang	$\rightarrow$ expansion and recollapse	A_- big crunch
		A_- big bang	$\rightarrow$ expansion and recollapse	B_- big crunch
		A_+ past infinity	$\rightarrow$ collapse	B_- big crunch

Figure 3.5: Possible evolutions of 1D systems according to the sign and the slope of the potential.

3.3. Two-dimensional phase-space

In what follows, we would like to perform the same study we have just seen but considering an additional component (whose density and pressure are denoted with ρ_γ and p_γ respectively) which is not explicitly coupled to the scalar field. It only enters the Friedmann constraint, which reads

$$H^2 = \frac{1}{3M_P^2}\left(\frac{\dot{\phi}^2}{2} + V(\phi) + \rho_\gamma\right) ,$$

ρ_γ obeying the continuity equation

$$\dot{\rho}_\gamma = -3H(\rho_\gamma + p_\gamma) \,. \tag{3.8}$$

We consider a barotropic fluid whose equation of state is $p_\gamma = (\gamma - 1)\rho_\gamma$; γ is simply a constant such that, for conventional fluids, $\gamma \in (0, 2)$. For instance, if we consider dust $\gamma = 1$ or for radiation we have $\gamma = 4/3$. The KG equation (2.26) still holds for the evolution of the scalar field.

The idea is to proceed following the same steps as before. Therefore, on top of the dimensionless variables x and y we had in Eqs. (3.3) and (3.4) respectively, we define a new one associated with ρ_γ:

$$w \equiv \frac{\sqrt{\rho_\gamma}}{\sqrt{3}M_P H}\,. \tag{3.9}$$

The evolution equations turn into an autonomous system given by

$$x' = -3x\left(1 - x^2 - \frac{\gamma}{2}w^2\right) \pm \lambda\sqrt{\frac{3}{2}}y^2\,, \tag{3.10}$$

$$y' = y\left(3x^2 - \lambda\sqrt{\frac{3}{2}}x + \frac{3\gamma}{2}w^2\right)\,, \tag{3.11}$$

$$w' = \frac{3}{2}w\left(-\gamma + 2x^2 + \gamma w^2\right)\,. \tag{3.12}$$

In addition, the Friedmann constraint becomes

$$x^2 \pm y^2 + w^2 = 1 \tag{3.13}$$

so that the system is reduced to a 2D phase-space corresponding to a unit sphere for $V \geq 0$ or to a hyperboloid for $V \leq 0$.
We will stick to the case $H > 0$, corresponding to the upper quadrant $y \geq 0$ and $w \geq 0$, noting that our system is symmetric under $t \to -t$, $H \to -H$, $y \to -y$ and $w \to -w$.

3.3.1 Critical points

Just like before, critical points are the ones for which $x' = y' = w' = 0$. One can check there are at most five fixed points: three are represented by $A_\pm$ and B we have seen before (clearly $w_i = 0, \quad i = A_\pm, B$ for all of them); on top of these, we have

- Fluid-dominated solution

  $$C = (0, 0, 1)$$

  i.e. only w_C is non-vanishing. This solutions is always present, irrespective of the potential.

- Fluid-potential-kinetic-scaling solution[3]

$$D = \left(\sqrt{\frac{3}{2}}\frac{\gamma}{\lambda}, \sqrt{\pm\frac{3}{2}\frac{(2-\gamma)\gamma}{\lambda^2}}, \sqrt{1-\frac{3\gamma}{\lambda^2}} \right)$$

  As we can see from y_D and w_D, this solution exists only for positive potentials which are sufficiently steep (in this case we mean $\lambda^2 > 3\gamma$).

3.3.2 Stability

If we consider the $w = 0$ subspace, the study of the stability of the points $A_\pm$ and B is the same as in the previous section. Instead, if we consider fluid perturbations, they evolve as $\delta w_i \propto e^{mN}$ where $m = 3(2x_i^2 - \gamma)/2$. This means:

- Stability of $A_\pm$ to fluid perturbations
  For $A_\pm$ we have $m = 3(2-\gamma)/2$. Being $\gamma < 2$, kinetic-dominated solutions are always unstable to fluid perturbations.

- Stability of B to fluid perturbations
  In this case, $m = (\lambda^2 - 3\gamma)/2$. This entails the kinetic-potential-scaling solution is stable for sufficiently flat potentials ($\lambda^2 < 3\gamma$), but unstable for sufficiently steep potentials.

- Stability of C and D
  The fluid-dominated solution has two eigenmodes of the kind $\delta x_i \propto e^{m_x N}$ and $\delta y_i \propto e^{m_y N}$, with $m_x = -3(2-\gamma)/2$ and $m_y = 3\gamma/2$. Hence, it is stable to kinetic energy perturbations being $\gamma < 2$, but it is unstable to potential energy perturbations, being $\gamma > 0$. We have a saddle point which is unstable to generic perturbations.
  Point D is always a stable late-time attractor when it exists [4].

3.3.3 Qualitative evolution in the phase-space

1. Flat positive potentials ($V > 0, \quad \lambda^2 < 3\gamma$)
   We have four critical points: $A_\pm$ are unstable repellors, C is the unstable saddle point and B is the stable late-time attractor. This means generic solutions start from the kinetic-dominate regime A_+ or A_- ending in the potential-kinetic scaling regime represented by B, as shown in Fig. 3.6. There is the possibility for such solutions to approach C in their way to the kinetic-potential-scaling solution.

[3]Hereafter we simply call it *scaling solution.*

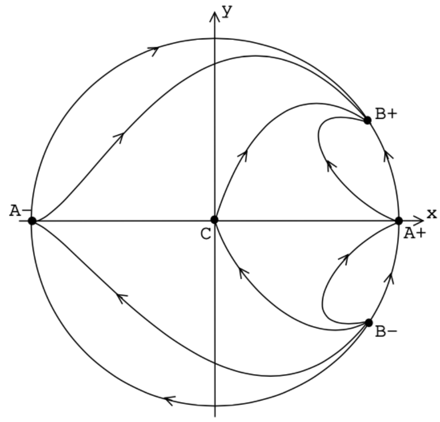

Figure 3.6: 2D phase-space for flat positive potentials.
© Copyright [13].

2. Intermediate positive potentials ($V > 0, \quad 3\gamma < \lambda^2 < 6$)
   All critical points are allowed here. Fig. 3.7 shows that generic solutions begin

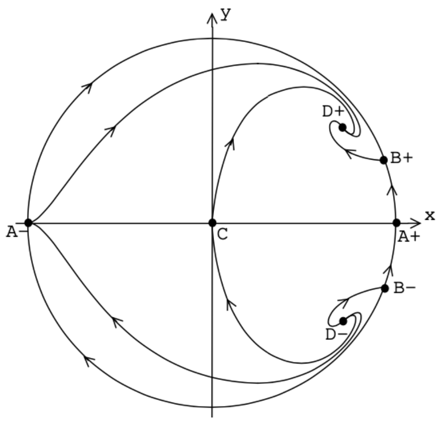

Figure 3.7: 2D phase-space for intermediate positive potentials.
© Copyright [13].

in the kinetic-dominated regime (A_+ or A_-), can approach either the fluid-dominated solution C or the kinetic-potential scaling solution B, which are both unstable, and eventually reach the scaling solution D at late times, which is a stable attractor.

3. Steep positive potentials ($V > 0, \quad \lambda^2 > 6$)
   Now the kinetic-potential-scaling solution is not present. We have only four critical points corresponding to $A_\pm$, C and D. $A_\pm$ are as usual unstable repellors, C is the unstable saddle point, while D is instead the stable late-time attractor. Thus, solutions start out kinetic-dominated and eventually

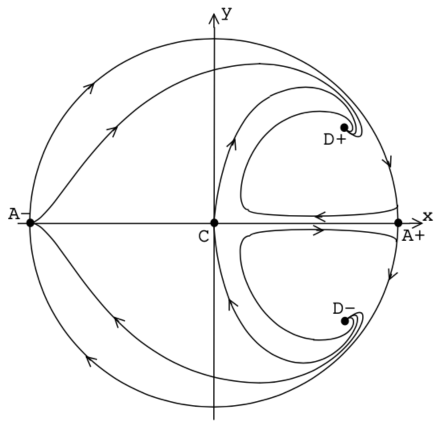

Figure 3.8: 2D phase-space for steep positive potentials.
© Copyright [13].

reach the scaling solution, approaching or not the fluid-dominated solution in their way towards D.

4. Flat negative potentials ($V < 0, \quad \lambda^2 < 6$)
   Now we have only three critical points at our disposal, that is to say $A_\pm$

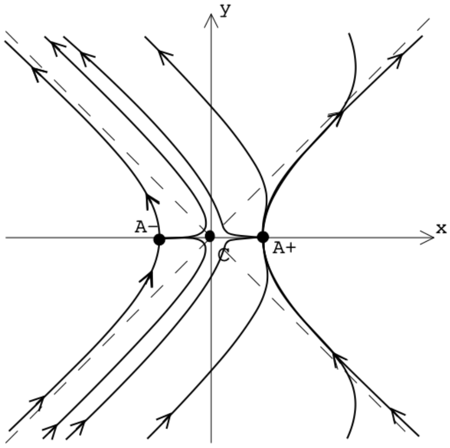

Figure 3.9: 2D phase-space for flat negative potentials.
© Copyright [13].

(unstable repellors) and the unstable C. As we can see from Fig. 3.9, generic solutions start out kinetic-dominated and go to infinity along $x = -y$. Then, they can either approach C or not, and eventually recollapse to A_+.

5. Steep negative potentials ($V < 0, \quad \lambda^2 > 6$)
   Finally, steep negative potentials enable the existence of four critical points. If we look at Fig. 3.10 we have the following situations: generic solutions begin either in the kinetic-dominated regime A_- (if $\dot{\phi} < 0$) or in the kinetic-potential-

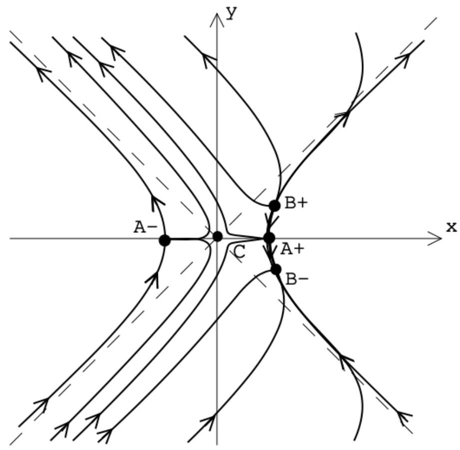

Figure 3.10: 2D phase-space for steep negative potentials.
© Copyright [13].

scaling regime B (if $\dot{\phi} > 0$); then, the former can approach the fluid-dominated solution C before going to infinity along $x = -y$ and recollapsing towards the late-time attractor B. Instead, the latter can approach both the fluid-dominated solution C and the kinetic-dominated solution A_+, which are both unstable, before going to infinity and recollapsing towards B.

3.4. Final considerations

Let us give a quick recap about the possible outcomes we have found. Basically, we have performed the study of the phase-space according to the nature of the exponential potential, which could be positive or negative, flat or steep.
In particular, we have seen how positive and sufficiently flat potentials are featured by a potential-kinetic scaling solution (i.e. B) were the contributions of the kinetic energy density and of the potential energy density remain proportional; they describe expanding cosmologies (or contracting cosmologies if we look at them in the lower plane). The potential-kinetic scaling solution does not show up for steep positive potentials, which are describing only expanding cosmologies.
The kinetic-potential-scaling solution is also missing for flat negative potentials, which are associated with a behaviour of the kind "Big Bang → expansion → recollapse → Big Crunch". Thus, for flat negative potentials we always have collapsing cosmologies.
However, negative potentials which are sufficiently steep present both expanding solutions (those starting close to the kinetic-pontential scaling solution and approaching at late times the kinetic solution) and Big Bang-Big Crunch solutions.

3.5. A "Cosmic No-Hair Theorem" for contracting cosmologies

An important matter when studying cosmologies with a Big Crunch/Big Bang transition is the behaviour of the Universe as it approaches the crunch. We are going to discuss the possible situations that can arise according to the value taken by ω in the equation of state (1.6). We will focus on a contracting Universe for which the transition Big Crunch/Big Bang occurs at $t = 0$, where $t \to 0^-$ is basically what we are intrested in eventually, i.e. the crunch. In other words, we consider the range $t \in (-\infty, 0^-]$ where the Universe is contracting towards $a \overset{t\to 0^-}{\longrightarrow} 0$. In particular, we will first discuss the curvature-free case and then we will briefly tell what happens when curvature is taken into account.

The first thing to point out is the form of the metric. A known result in literature is that the dynamics of the metric near the crunch are *ultralocal*: this means that the evolution of adjacent spatial point decouples since spatial gradients increase more slowly than other terms in the equations of motion. From a mathematical point of view, this translates into the following form of the metric near the singularity and at a fixed spatial coordinate $\mathbf{x}_0$

$$ds^2 = -dt^2 + a^2(t, \mathbf{x}_0) \sum_i e^{2\beta_i(t,\mathbf{x}_0)} \left(\sigma^{(i)}(\mathbf{x}_0)\right)^2 \tag{3.14}$$

with the constraint

$$\sum_{i=1}^{3} \beta_i = 0\,. \tag{3.15}$$

The metric in Eq. (3.14) is a Kasner-like metric. We now suppress the dependence on $\mathbf{x}_0$ for simplicity: $\sigma^{(i)}$ are linearly independent one-forms; $a(t)$ is a common scale factor, similarly to a FLRW metric, but the effective scale factor along the i-th direction is $a\, e^{\beta_i}$, so that each β_i describes the contraction or expansion of the associated direction with respect to the overall volume contraction. Therefore, we are taking into account a general anisotropic contraction, and the dynamics of an inhomogeneous universe at a fixed spatial point can be approximated, close to the singularity, by that of a homogeneous, even though curved and anisotropic, universe. $\sigma^{(i)}$ and $a\, e^{\beta_i}$ account for differences in curvature and anisotropy at different $\mathbf{x}_0$. The freedom to rescale each σ enables us to pick a time t_0 for which $a(t_0) = 1$ and $\beta_i(t_0) = 0$. When we meet a quantity with a subscript zero, they will refer to their values at t_0.

Before we move on to study the curvature-free case, there is one more issue to point out: if we look at the evolution equation (1.8) of the energy density for a component with equation of state $p = \omega\rho$, for an expanding universe the component with the largest value of ω redshifts away more slowly that the others so that it dominates in the end. On the other hand, for a contracting universe, the component with the largest value of ω will take over. This let us safely ignore any other perfect fluid with $\omega_i < \omega$ and consider just the one which dominates near the crunch.

3.5.1 The curvature-free case

Let us first consider the case of flat spatial 3-surfaces. In this case, Einstein equations yield

$$3\left(\frac{\dot{a}}{a}\right)^2 - \frac{1}{2}\left(\dot{\beta}_1^2 + \dot{\beta}_2^2 + \dot{\beta}_3^2\right) = \rho\,, \tag{3.16}$$

$$\ddot{\beta}_i + 3\frac{\dot{a}}{a}\dot{\beta}_i = 0\,. \tag{3.17}$$

Now, if we integrate Eq. (3.17) we find

$$\dot{\beta}_i = c_i a^{-3} \tag{3.18}$$

for which the constraint (3.15) becomes

$$c_1 + c_2 + c_3 = 0\,. \tag{3.19}$$

Hence, it is easy to see how Eq. (3.16) becomes the Friedmann equation

$$3\left(\frac{\dot{a}}{a}\right)^2 = \rho(a) + \frac{\sigma^2}{a^6} = \frac{\rho_0}{a^{3(1+\omega)}} + \frac{\sigma^2}{a^6}\,, \tag{3.20}$$

where the curvature term is absent ($k = 0$) but we have a so called anisotropy term σ^2/a^6 with

$$\sigma^2 \equiv \frac{1}{2}(c_1^2 + c_2^2 + c_3^2)\,. \tag{3.21}$$

As we will see, the effective contribution of anisotropy is a different expansion/contraction in different spatial directions. Let us consider the fractional energy densities

$$\Omega_\rho = \frac{\rho(a)}{\rho(a) + \sigma^2/a^6}\,, \tag{3.22}$$

$$\Omega_\sigma = \frac{\sigma^2/a^6}{\rho(a) + \sigma^2/a^6}\,, \tag{3.23}$$

representing respectively the contribution of the perfect fluid and anisotropy to the critical density.

One can now find an expression for $\beta_i(a)$ starting from Eq. (3.18) and using Eq. (3.20):

$$\beta_i(a) = c_i\sqrt{3}\int_a^1 \frac{da'}{a'}\left(\rho(a')a'^6 + \sigma^2\right)^{-1/2} , \tag{3.24}$$

where the endpoints of integration are chosen so as to have $\beta_i(1) = 0$. With this at hand, one can study different situations related to the value taken by ω.

$\omega < \mathbf{1}$

In this case, $\rho(a)a^6 \sim a^2$ so it is negligible in Eq. (3.24) as $a \to 0$. This means the solution corresponds to the vacuum Kasner Universe during contraction given by

$$a(t) = \left(\frac{t}{t_0}\right)^{1/3} , \tag{3.25}$$

$$\beta_i(t) = \frac{c_i}{\sigma\sqrt{3}}\ln\left(\frac{t}{t_0}\right) . \tag{3.26}$$

This Kasner Universe is parametrised by the so called Kasner exponents

$$p_i = \frac{1}{3} + \frac{c_i}{\sigma\sqrt{3}} \tag{3.27}$$

so that the effective scale factors are

$$a\, e^{\beta_i} = \left|\frac{t}{t_0}\right|^{p_i} . \tag{3.28}$$

Therefore, we see how the Kasner exponent p_i basically describes how the Universe is expanding/contracting in the i-th direction, and in turn this is strictly connected to the anisotropy contribution expressed by the presence of σ in Eq. (3.27).
Note that the relations (3.19) and (3.21) now read respectively

$$p_1 + p_2 + p_3 = 1 \tag{3.29}$$

$$p_1^2 + p_2^2 + p_3^2 = 1 , \tag{3.30}$$

which are the so called *Kasner conditions*. They are related to the *Kasner circle*, i.e. the intersection between the *Kasner plane* and the *Kasner sphere* (with unit radius for this particular case where $\omega < 1$). The Kasner circle contains all the allowed valued of p_i. If we look at Figure 3.11, for $\omega < 1$ the Kasner circle is the outermost one, associated with $\Omega_\sigma = 1$. On that particular circle, the black dots correspond to the case where one single Kasner exponent is equal to one and all the others are vanishing; the dashed part of the circle contains points where one Kasner exponent is negative, meaning the direction associated with it is not contracting but expanding. Therefore, we have an overall contraction, but a single scale factor related to the negative Kasner exponent is expanding, so that the Universe becomes increasingly anisotropic as we approach the crunch. The isotropic solution where all the $p_i = 1/3$ is indeed not compatible with the Kasner conditions.

$\omega = \mathbf{1}$

By looking at the evolution equation (1.8), for $\omega = 1$ we have $\rho \sim a^{-6}$.[4] This is telling us that the matter density and the anisotropy term scale with the same power of the scale factor a. Solutions for a and β_i in this case are given by

$$a(t) = \left(\frac{t}{t_0}\right)^{1/3}, \tag{3.31}$$

$$\beta_i(t) = \frac{c_i}{\sqrt{3(\sigma^2 + \rho_0)}} \ln\left(\frac{t}{t_0}\right). \tag{3.32}$$

It is similar to the $\omega < 1$ case so we define the Kasner exponents as

$$p_i = \frac{1}{3} + \frac{c_i}{\sigma\sqrt{3}}\left(1 + \frac{\rho_0}{\sigma^2}\right)^{-1/2}. \tag{3.33}$$

However, Kasner conditions here are different and given by

$$p_1 + p_2 + p_3 = 1 \tag{3.34}$$

$$p_1^2 + p_2^2 + p_3^2 = 1 - q^2 = \frac{1}{3} + \frac{2}{3}\Omega_\sigma\,, \tag{3.35}$$

where

$$q^2 \equiv \frac{2}{3}(1 - \Omega_\sigma) = \frac{2}{3}\frac{\rho_0}{\sigma^2 + \rho_0}. \tag{3.36}$$

So, for $\omega = 1$ we have different Kasner circles according to the value of Ω_σ. Let us look at Figure 3.11: the degenerate solution is the innermost circle, i.e. the point corresponding to the perfectly isotropic case where $\Omega_\sigma = 0$. In fact, the Kasner conditions here are compatible with $p_i = 1/3 \;\; \forall i$. Then, as long as $\Omega_\sigma < 1/4$ (corresponding to the white region but only within the larger solid circle inscribed in the triangle) all the Kasner exponents are positive and so the Universe contract smoothly to the crunch but the effective scale factors decrease at different rates, since Kasner exponents do not take the same value. For $\Omega_\sigma > 1/4$ (see for example the third largest circle, which shows solid parts inside the white region but also dashed parts outside) some points on the Kasner circle have one negative Kasner

[4] Keep in mind that ρ_0 appearing in Eq. (1.8) is not the same we are dealing with in this section. However, what we are interested in, as far as Eq. (1.8) is concerned, is just the scaling of ρ with a.

exponent, so we have the same situation as the $\omega < 1$ case. Therefore, we still have, in general, a smooth but anisotropically contraction to the crunch, except for the special case $\Omega_\sigma = 0$.

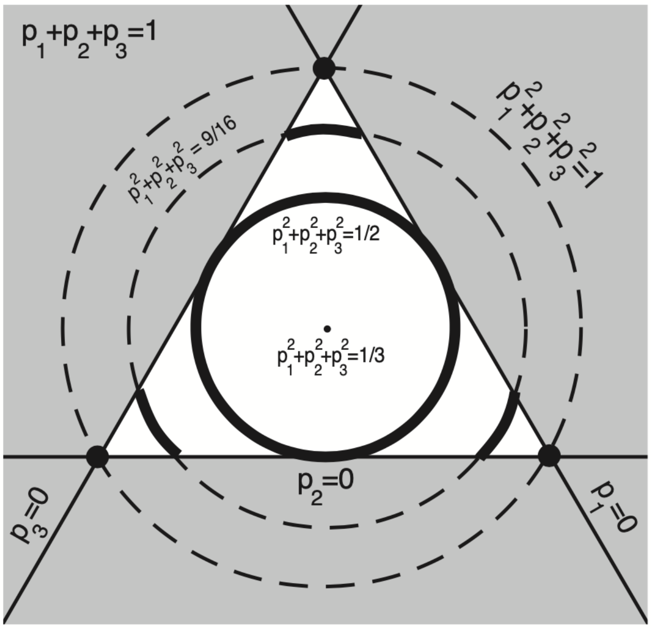

Figure 3.11: The Kasner plane represented by $\sum_i p_i = 0$ and the itersections, called Kasner circles, with different spheres $\sum_i p_i^2 = 1 - q^2$. The vacuum Kasner solution corresponds to $\Omega_\sigma = 1$, i.e. $q = 0$, which is the outermost circle. Other circles are relevant for the case $\omega = 1$ and $\Omega_\sigma < 1$. White regions are associated with all positive Kasner exponents, whereas in the grey regions one exponent is negative.
© Copyright [5].

$\omega > \mathbf{1}$

If $\omega > 1$ then $\rho(a) \sim a^{-x}$ with $x > 6$ so it dominates over the the anisotropic part and $\Omega_\rho \to 1$ as $a \to 0$. The solution is

$$a(t) = \left(\frac{t}{t_0}\right)^{\frac{2}{3(1+\omega)}}, \tag{3.37}$$

$$\beta_i(t) = c_i \frac{2}{\sqrt{3\rho_0}} \frac{1}{\omega - 1} \left[\left(\frac{t}{t_0}\right)^{\frac{\omega-1}{\omega+1}} - 1\right]. \tag{3.38}$$

From Eq. (3.38) we see how $\beta_i \sim t^\alpha$ with $\alpha > 0$ for $\omega > 1$. As a consequence, when we approach the crunch β_i tends to a constant, so that the Universe becomes isotropic. This is what we call a "cosmic no-hair theorem" for universes with no spatial curvature: when $\omega < 1$ the Universe is more and more anisotropic as we get closer to the crunch (i.e. $\Omega_\sigma \to 1$ as $a \to 0$). For $\omega = 1$, Ω_σ remains fixed; however, there is an anisotropically but still smooth contraction towards the crunch, where we mean there is no jump between one Kasner-like solution to another (this is known as *mixmaster behaviour*, and it is experienced when curvature is taken into account). Finally, for $\omega > 1$ the initial anisotropy disappears as we approach the crunch, where the Universe becomes isotropic.

3.5.2 Curvature

When we consider the presence of curvature, things get messier. We will not go into details just list what happens for different values of ω.
For $\omega < 1$ the spatial curvature is responsible for a chaotic mixmaster behaviour where the Universe jumps an infinite numer of times between different Kasner-like epochs. The Universe becomes extremely inhomogeneous as we approach $a \to 0$.
The chaotic behaviour is softened when $\omega = 1$. In particular, if $\Omega_\sigma < 1/4$ some choices of the p_i have one $p_i < 0$ and the system still jumps between different p_i's; we call these points *unstable*. However, the number of jumps now is finite, and the Universe hits a point belonging to the open subset of stable p_i. Starting from here, there is a smooth contraction, with no more jumps, towards a stable point as $a \to 0$. These models are called *non-chaotic*.
As for the curvature-free case, when $\omega > 1$ the curvature does not affec the contraction, and the solution converges to the isotropic one. Thus, a generalisation of the "cosmic no-hair theorem" which includes the presence of curvature is possible: an initially anisotropic and inhomogeneous universe with spatial curvature collapses to a flat, homogeneous and isotropic universe if it contains energy with $\omega > 1$, whereas it collapses to a flat, homogeneous but anisotropic universe if $\omega = 1$. For $\omega < 1$ the universe is highly inhomogeneous and the no-hair theorem does not hold anymore.

CHAPTER 4

STATIC SPHERICALLY SYMMETRIC SOLUTION WITH AN EXPONENTIAL POTENTIAL

In the previous chapter we have studied the properties of a cosmological solution associated with an exponential potential whose sign is left arbitrary. This fact, along with the slope of the potential (i.e. the value taken by λ), produces several physical scenarios that we have discussed.
Now we consider again a scalar field with a KG kinetic term and an exponential potential of the kind (3.1) but in a static and spherically symmetric (SSS) spacetime. We will find the solution to Einstein equations. As expected, since we are dealing with a SSS spacetime, we get the definition of its related horizon. Therefore, we will check it is a coordinate singularity (just like for the Schwarzschild radius) and we will eventually discuss the properties of our solution.

4.1. Equations of motion and their solution in a static and spherically symmetric spacetime

Let us consider the following Lagrangian for our model

$$\mathcal{L} = -\frac{\epsilon}{2}\nabla_\mu\phi\nabla^\mu\phi - V_0 e^{-\lambda\frac{\phi}{M_P}} \, . \tag{4.1}$$

Clearly, for a scalar field ϕ the covariant derivative reduces to the usual partial derivative, so Eq. (4.1) is nothing else than Eq. (3.2) up to a sign represented by $\epsilon = \pm 1$, where $\epsilon = +1$ corresponds to the standard normalization for the kinetic term and $\epsilon = -1$ to the non-standard normalization. The sign of the pontential is still left arbitrary.

Now, our goal is to find the solution to equations of motion in a SSS spacetime. To this end, we write the metric as follows

$$ds^2 = -e^{\nu(r)}dt^2 + e^{\lambda(r)}dr^2 + r^2 d\Omega^2 \,, \tag{4.2}$$

where $d\Omega^2 = d\theta^2 + \sin^2\theta \, d\varphi^2$ and $e^{\nu(r)}$, $e^{\lambda(r)}$ are unknown functions to be determined once we solve Einstein equations. With this at hand, equations of motion read

$$e^{-\lambda}\left[\frac{1}{r^2} - \frac{\lambda'}{r}\right] - \frac{1}{r^2} = -\chi\left[\frac{\epsilon}{2}e^{-\lambda}\phi'^2 + V(\phi)\right] \quad , \tag{4.3}$$

$$\frac{\lambda' + \nu'}{r} = \chi\,\epsilon\,\phi'^2 \quad , \tag{4.4}$$

$$\phi'' - \frac{1}{2}\phi'\left(\lambda' - \nu' - \frac{4}{r}\right) - \epsilon\,\partial_\phi V(\phi)e^{\lambda} = 0 \quad , \tag{4.5}$$

where $\chi = 8\pi G$. The solution is then given by[1]

$$\begin{aligned} e^{\nu(r)} &= \left(\frac{r}{r_0}\right)^{2(1-\gamma)/\gamma} \frac{1}{2\gamma - 1}\left[1 + (2\gamma - 1)\frac{C}{r_0}\left(\frac{r_0}{r}\right)^{1/\gamma}\right] \\ &= \left(\frac{r}{r_0}\right)^{2(1-\gamma)/\gamma} \frac{1}{2\gamma - 1}\left[1 - (2\gamma - 1)\frac{2M}{r_0}\left(\frac{r_0}{r}\right)^{1/\gamma}\right] , \end{aligned} \tag{4.6}$$

$$\begin{aligned} e^{\lambda(r)} &= \frac{2\gamma - 1}{\gamma^2}\left(1 + (2\gamma - 1)\frac{C}{r_0}\left(\frac{r_0}{r}\right)^{1/\gamma}\right)^{-1} \\ &= \frac{2\gamma - 1}{\gamma^2}\left(1 - (2\gamma - 1)\frac{2M}{r_0}\left(\frac{r_0}{r}\right)^{1/\gamma}\right)^{-1} \end{aligned} \tag{4.7}$$

and

$$\phi(r) = \pm a(\gamma)\ln(r/r_0) + \phi(r_0) \,, \tag{4.8}$$

where $C = -2M$ is a dimensionful constant $[C] = [L]$, γ is a dimensionless parameter whereas $[r_0] = [L]$. We rewrite the considered potential for ϕ as

$$V(\phi) = V_0 e^{2b\,\phi} \,. \tag{4.9}$$

[1] The most general solution with a potential of the kind (3.1) is not known. However, if we assume $e^{\lambda(r)} \cdot e^{\nu(r)}$ to be a power of r, then we can find our solution.

The quantity $a(\gamma)$ is defined by

$$a(\gamma) = [2(1-\gamma)/(\epsilon\chi\gamma)]^{1/2} \tag{4.10}$$

Furthermore, in order for Eqs. (4.6)-(4.8) to be solutions, the following constraint on b

$$\mp b\, a(\gamma) = 1 \tag{4.11}$$

and on V_0

$$V_0 e^{2b\,\phi(r_0)} = \frac{1}{\chi\, r_0^2} \frac{(\gamma-1)}{(2\gamma-1)} \tag{4.12}$$

have to be satisfied.
We also note that our solution can be written as

$$ds^2 = -U(r)dt^2 + \frac{1}{U(r)\,\gamma^2}\left(\frac{r}{r_0}\right)^{2(1-\gamma)/\gamma} dr^2 + r^2 d\Omega^2\,. \tag{4.13}$$

with

$$\begin{aligned} U(r) &= \left(\frac{r}{r_0}\right)^{-2+1/\gamma}\left(\frac{1}{2\gamma-1}\left(\frac{r}{r_0}\right)^{1/\gamma} + \frac{C}{r_0}\right) \\ &= \left(\frac{r}{r_0}\right)^{2(1-\gamma)/\gamma} \frac{1}{2\gamma-1}\left[1 + (2\gamma-1)\frac{C}{r_0}\left(\frac{r_0}{r}\right)^{1/\gamma}\right] \end{aligned} \tag{4.14}$$

Our solution can hide a horizon, which is not something strange when we deal with a SSS spacetime. Therefore, let us define it as

$$r_S \equiv r_0\left[\frac{2M}{r_0}(2\gamma-1)\right]^{\gamma} \tag{4.15}$$

so that we can write Eqs. (4.6) and (4.7) respectively as

$$e^{\nu(r)} = \left(\frac{r}{r_0}\right)^{2(1-\gamma)/\gamma} \frac{1}{2\gamma-1}\left[1 - \left(\frac{r_S}{r}\right)^{1/\gamma}\right] \tag{4.16}$$

and

$$e^{\lambda(r)} = \frac{2\gamma-1}{\gamma^2}\left(1 - \left(\frac{r_S}{r}\right)^{1/\gamma}\right)^{-1}\,. \tag{4.17}$$

Therefore, it is natural to check whether our solution is regular or not near the horizon itself, at least for the values of the parameter γ for which it exits (see

Section 4.4), that is $1/2 < \gamma < 1$. Therefore, let us stick to this subset of γ for the time being.

4.1.1 Curvature invariants

We also give the expression for curvature invariants. In particular, we have:

- *Ricci scalar* $R = R^{\alpha}_{\alpha}$

$$R = \frac{2(\gamma-1)}{r^2}\left(\frac{2-\gamma}{2\gamma-1} - \frac{C\gamma}{r_0}\left(\frac{r_0}{r}\right)^{1/\gamma}\right). \tag{4.18}$$

- *Ricci square* $R^2 = R^{\alpha\beta}R_{\alpha\beta}$

$$R^2 = \frac{4(\gamma-1)^2}{r^4}\left[\frac{1}{4} + \frac{3}{4(2\gamma-1)^2} + \frac{C\gamma}{r_0}\left(\frac{r_0}{r}\right)^{2/\gamma}\left(\frac{C\gamma}{r_0} + \left(\frac{r}{r_0}\right)^{1/\gamma}\right)\right]. \tag{4.19}$$

- *Riemann square* or *Kretschmann invariant* $K = R^{\alpha\beta\mu\nu}R_{\alpha\beta\mu\nu}$

$$\begin{aligned} K = \frac{4}{r^4(1-2\gamma)^2}&\left[\left(\frac{r_0}{r}\right)^{2/\gamma}\left(\left(\frac{C}{r_0}\right)^2(1-2\gamma)^2\gamma^2(2+\gamma(-6+7\gamma))+\right.\right.\\ &+2\frac{C}{r_0}(-1+\gamma)\gamma(2\gamma-1)(1+\gamma(-6+7\gamma))\left(\frac{r}{r_0}\right)^{1/\gamma}\\ &\left.\left.+(\gamma-1)^2(2+\gamma(-6+7\gamma))\left(\frac{r}{r_0}\right)^{2/\gamma}\right)\right]. \end{aligned} \tag{4.20}$$

Note that in the limit $\gamma \to 1$ the Schwarzschild invariants are recovered

$$R \xrightarrow{\gamma\to 1} 0 \tag{4.21}$$

$$R^2 \xrightarrow{\gamma\to 1} 0 \tag{4.22}$$

$$K \xrightarrow{\gamma\to 1} 12\,C^2/r^6 \tag{4.23}$$

4.2. Relation to Mann solution

In what follows we are going to show how our solution belongs to a class of charged dilaton BH solution studied in [3] by Mann and collaborators. In particular, Mann solution is a charged BH solution with an anusual asymptotic behaviour which is neither flat nor dS.
Mann solution is given by

$$ds^2 = -U_1(r)dt^2 + \frac{dr^2}{U_1(r)} + R^2(r)d\Omega^2 \tag{4.24}$$

with

$$R(r) = \alpha r^N \tag{4.25}$$

where α is a dimensionful constant such that $[\alpha] = [L^{1-N}]$. For $Q = 0$,

$$U_1(r) = r^{\frac{2a^2}{1+a^2}} \left(\frac{1+a^2}{(1-a^2)\alpha^2} - \frac{2(1+a^2)M}{\alpha^2 r} \right) . \tag{4.26}$$

N is defined through the relation

$$N = \frac{1}{1+a^2} . \tag{4.27}$$

Therefore

$$U_1(r) = r^{2(1-N)} \left(\frac{1}{(2N-1)\alpha^2} - \frac{2M}{\alpha^2 r N} \right) . \tag{4.28}$$

Using $r = (\frac{1}{\alpha}R)^{1/N}$ and calling $C = -2M$ we have

$$\begin{aligned} U_1(R) &= R^{2(1-N)/N} \frac{1}{\alpha^{2(1-N)/N}} \left[\frac{1}{(2N-1)\alpha^2} + \frac{C\alpha^{1/N}}{\alpha^2 N R^{1/N}} \right] \\ &= R^{2(1-N)/N} \frac{1}{2N-1} \frac{1}{\alpha^{2/N}} \left[1 + \frac{2N-1}{N} \frac{C\alpha^{1/N}}{R^{1/N}} \right] . \end{aligned} \tag{4.29}$$

Given

$$dr^2 = \frac{1}{N^2} R^{2(1-N)/N} \frac{1}{\alpha^{2/N}} dR^2$$

We finally have

$$ds^2 = -U_1(R)dt^2 + \frac{1}{U_1(R)N^2} R^{2(1-N)/N} \frac{1}{\alpha^{2/N}} dR^2 + R^2 d\Omega^2 \tag{4.30}$$

Upon renaming $N \to \gamma$, $R \to r$ and $\alpha \to r_0^{1-\gamma}$ we get Eq. (4.13) up to a $\frac{1}{N}$ factor present in the last term in Eq. (4.29). The reader can easily check by substitution that it still satisfies equations of motion.

4.3. Kruskal extension

In GR, *Kruskal coordinates* represent a set of coordinates whose purpose is to show that the Schwarzschild radius is just a coordinate singularity. In other words, by changing coordinates in the Schwarzschild solution, one is able to show that there is no singularity at all in $r = R_S$, where R_S is the Schwarzschild radius. The new set of coordinates where this happens is precisely the Kruskal one.[2]

The aim of this section is to show the regularity of our solution near the horizon r_S starting from Mann solution (4.24). To this purpose, following the same procedure as for the Schwarzschild solution, we are going to find the Kruskal extension for ours, proving in an alternative way Mann's thesis.

First of all, we find radial null directions by setting $ds^2 = 0$ and $\theta, \phi =$ const. in Eq. (4.24). We get

$$dt = \pm \frac{dr}{U_1(r)} \equiv \pm dr^* \,. \tag{4.31}$$

Let us rewrite $U_1(r)$ in Eq. (4.28) as

$$U_1(r) = r^{2(1-N)} \frac{1}{(2N-1)\alpha^2} \left(1 - \frac{r_S}{r}\right) \tag{4.32}$$

where

$$r_S \equiv \frac{2M(2N-1)}{N} = -\frac{C(2N-1)}{N} \,.$$

Then, we expand $U_1(r)$ about r_S as

$$U_1(r) \simeq \left.\frac{dU_1(r)}{dr}\right|_{r_S} (r - r_S) \,.$$

We compute $U_1'(r)$:

$$\begin{aligned} \frac{dU_1(r)}{dr} &= \frac{1}{(2N-1)\alpha^2} \left[2(1-N) r^{1-2N} \left(1 - \frac{r_S}{r}\right) + r^{2(1-N)} \left(\frac{r_S}{r^2}\right)\right] \\ &= \frac{1}{(2N-1)\alpha^2} \left[2(1-N) r^{1-2N} \left(1 - \frac{r_S}{r}\right) + r_S\, r^{-2N}\right] \end{aligned}$$

Hence

$$U_1(r) \simeq \frac{r_S^{1-2N}}{(2N-1)\alpha^2} (r - r_S) \,. \tag{4.33}$$

Considering the definition of the coordinate r^* in Eq. (4.31), upon integration we have

$$r^* = \frac{(2N-1) r^{2N} \alpha^2 \, {}_2F_1(1, 2N; 1+2N; r/r_S)}{2N r_S}$$

where ${}_2F_1(a, b; c; z)$ is the *Gaussian* or *ordinary hypergeometric function* whose expression is

$${}_2F_1(a, b; c; z) = 1 + \frac{ab}{c}\frac{z}{1!} + \frac{a(a+1)b(b+1)}{c(c+1)}\frac{z^2}{2!} + \dots$$

[2]To be more precise, the Kruskal extension is not the only one which enables us to solve the problem of the singularity in $r = R_S$. Kruskal coordinates are related to Eddington-Finkelstein coordinates which are null coordinates, so they are associated with propagation of light. On the other hand, one can look, for example, at the *Painlevé-Gullstrand coordinates*, which are instead based on timelike geodesic observers.

For the sake of simplicity, we adopt the approximation of $U_1(r)$ in Eq. (4.33) in order to find an easier formulation of the Kruskal coordinates. Therefore, we get

$$r^* \simeq \frac{(2N-1)\alpha^2}{r_S^{1-2N}} \ln(r - r_S)\,. \tag{4.34}$$

We then define the Eddington-Finkelstein (E-F) coordinates u and v through the relations

$$t = \frac{u+v}{2} \qquad r^* = \frac{v-u}{2}$$

so that

$$dt = \frac{du+dv}{2} \qquad dr^* = \frac{dv-du}{2}$$

i.e.

$$dr \simeq \frac{r_S^{1-2N}}{(2N-1)\alpha^2}(r - r_S)\frac{dv-du}{2}\,.$$

These coordinates provides us with the double-null form of Mann solution

$$ds^2 = -U_1(r)dudv + r^2(u,v)d\Omega^2\,.$$

Now, in order to find the Kruskal extension, we need the surface gravity κ. Therefore, we consider the Killing vector associated with time-translation invariance $\xi^\mu = (1,0,0,0)$, whose norm is given by $\xi^\mu\xi_\mu = g_{00}\xi^0\xi^0 = -U_1(r)$. Then, we study the following vector:

$$l_\mu = \left(0, \partial_r(\sqrt{-U_1(r)}), 0, 0\right) = \left(0, \sqrt{\frac{r^{1-2N}(r_S - r)}{(2N-1)\alpha^2}}\frac{[-2(N-1)r + (2N-1)r_S]}{2r(r_S - r)}, 0, 0\right)\,.$$

Its norm is

$$l_\mu l^\mu = g^{rr}(l_r)^2 = -\frac{r^{-4N}[2(N-1)r + (1-2N)r_S]^2}{4(1-2N)^2\alpha^4}\,.$$

Thus, the surface gravity is given by[3]

$$\kappa = \sqrt{|l_\mu l^\mu|}\Big|_{\text{horizon}} = \sqrt{\frac{r_S^2(-2+2N+1-2N)^2}{4r_S^{4N}(1-2N)^2\alpha^4}} = \frac{r_S^{1-2N}}{2(2N-1)\alpha^2}\,. \tag{4.35}$$

At this stage, we are able to write down the Kruskal coordinates as

$$U = -\frac{1}{\kappa}e^{-\kappa u} \qquad V = \frac{1}{\kappa}e^{\kappa v}$$

[3]Recall that the horizon is at $r = r_S$ and that $1/2 < N < 1$ (see Sec. 4.4).

and the Kruskal extension is obtained starting from the E-F double-null form as

$$ds^2 = -U_1(r)\frac{du}{dU}\frac{dv}{dV}dUdV + r^2(U,V)d\Omega^2\,,$$

where

$$\frac{du}{dU}\frac{dv}{dV} = e^{-\kappa(v-u)} = e^{-2\kappa r^*} \simeq \exp\left\{\ln\left[(r-rs)^{-2\kappa\frac{\alpha^2(2N-1)}{r_S^{1-2N}}}\right]\right\} = (r-r_S)^{-1}\,.$$

Thus, considering the approximation (4.33) and the above result, the Kruskal extension turns out to be

$$ds^2 = -\frac{r_s^{1-2N}}{(2N-1)\alpha^2}dUdV + r^2(U,V)d\Omega^2 \tag{4.36}$$

which clearly holds only near the horizon but shows explicitly that the solution (4.24) is regular at $r = r_S$.

4.4. Parameter Analysis

Since we are complying with the signature $(-,+,+,+)$, ϵ must be positive so as to have the standard kinetic term in our Lagrangian (4.1). Now, from Eqs. (4.10) and (4.11) we have

$$b^2 = \epsilon\,\frac{\chi\,\gamma}{2(1-\gamma)}\,.$$

In order to keep $\epsilon > 0$, since $b^2 > 0$ we find that $0 < \gamma < 1$. This range in γ can be further divided depending on the sign of V_0. From Eq. (4.12) we can see that $V_0 \propto (\gamma-1)/(2\gamma-1)$; hence, for $0 < \gamma < 1/2$ we have that $V_0 > 0$ and for $1/2 < \gamma < 1$ we have $V_0 < 0$.
So, $1/2 < \gamma < 1$ entails $V_0 < 0$ and our solution is a BH. Conversely, if we consider $0 < \gamma < 1/2$ we have a positive potential. In this case, $2\gamma - 1 \in (-1, 0)$ which means $2\gamma - 1 < 0$. As a consequence, $-(r_S/r)^{1/\gamma}$ in our solution is a positive quantity. In short, this implies there is no horizon at all, and $r = 0$ becomes a naked singularity. This is confirmed by [3] (see the case $a^2 > 1 \Leftrightarrow 0 < N < 1/2$).

4.5. Comparison between SSS solution and de Sitter Universe

We would like to figure out whether our SSS solution is the dS Universe up to a change of coordinates or an independent solution. To this end, we shall consider a quantity which does not vary under a coordinate transformation, that is a scalar.

In particular, we will compare the Ricci scalar of the dS solution to the one related to our SSS solution given in Eq. (4.18) (henceforward we call this $R_{\rm SSS}$).
For a dS Universe, the line element is given by

$$ds^2 = -dt^2 + e^{2H_0 t}\left(dr^2 + r^2 d\Omega^2\right) \,. \tag{4.37}$$

We are considering a dS universe since the previous line element can be recast in a static form [8]

$$ds^2 = -(1 - H_0^2 \bar{r}^2) d\bar{t}^2 + \frac{d\bar{r}^2}{1 - H_0^2 \bar{r}^2} + \bar{r}^2 d\Omega^2 \,. \tag{4.38}$$

where the transformation between the two line elements is

$$r = e^{H_0 \bar{t}} \frac{\bar{r}}{\sqrt{1 - \bar{r}^2 H_0^2}} \,, \qquad t = \bar{t} + \frac{1}{2H_0} \ln\left(1 - H_0^2 \bar{r}^2\right) \,.$$

Now, irrespective of the coordinates we use to write the dS line element, the Ricci scalar is given by

$$R_{\mathring{dS}} = 12 H_0^2 \,. \tag{4.39}$$

4.6. Comparison between SSS solution and the stable collapsing cosmology

To conclude, we would like to check if there is the possibility for our solution to be the stable collapsing FLRW as seen by another observer. We adopt the same procedure as for the dS Universe in the previous section.
The expression for the Ricci scalar is given by

$$R_{\rm FLRW} = 6\left(\dot{H} + 2H^2\right) = 6\left(\frac{\ddot{a}}{a} + \frac{\dot{a}^2}{a^2}\right) \,. \tag{4.40}$$

For a contracting cosmology, we shall consider $a(t) \sim |t|^p$ with $t \in (-\infty, 0^-]$ where $t = 0^-$ corresponds to the crunch. Hence, $a(t) \sim (-t)^p$. Thus, Eq. (4.40) reads

$$R^{\rm (contr)}_{\rm FLRW} = 6\frac{2p^2 - p}{t^2} \,. \tag{4.41}$$

The sign of this scalar depends on the value taken by p. In particular, for $p < 1/2$ Eq. (4.41) is negative, so its sign is the same as the Ricci scalar for our SSS solution. Conversely, for $p > 1/2$ the sign is positive.
Thus, we can safely say that for $p > 1/2$ our SSS solution is independent of the stable contracting FLRW solution, but for $p < 1/2$ it has to be explicitly checked. In particular, the relation between p and λ is $p = 2/\lambda^2$; $\lambda^2 < 6$ corresponds to

negative potentials associated with contracting cosmologies, i.e. $p < 1/3$. Therefore, the regime $p < 1/2$ contains the whole regime of stable collapsing solutions, and so it requires a further investigation.

CHAPTER 5

CONCLUSIONS AND OUTLOOKS

To summarize, we have seen how a scalar field with an exponential potential provides us with several different physical cosmologies which depend both on the sign and the exponent of the potential itself. In particular it is known that a positive (negative) and sufficiently flat (steep) exponential potential lead to stable expanding (contracting) cosmologies. This is the main toy-model for power-law inflation (ekpyrotic Universe).

It is therefore interesting to study in a complementary perspective a static and spherically symmetric spacetime, always with a scalar field with an exponential potential. By solving Einstein equations we confirm two possible cases depending on the parameter γ, and so on the sign of the potential: a naked singularity for $\gamma \in (0, 1/2)$, which corresponds to a positive potential, and a BH solution for $\gamma \in (1/2, 1)$ associated with a negative potential. We checked that our BH solution belongs to a class of charged dilaton BH solution with an unusual asymptotic behaviour obtained in [3]. We further confirmed, via the Kruskal extension, the regularity of the metric near the horizon. We have then demonstrated explicitly that this BH solution is not a coordinate transformation of the de Sitter Universe, whereas there is a range of the power-law exponent p for which a connection between our SSS solution and the stable collapsing FLRW solution might exist.

In the future it would be interesting to understand if this BH solution has phenomenological implications in the context of the ekpyrotic proposal or if it is nothing else than a coordinate transformation of the stable contracting cosmology.

APPENDIX A

CONNECTING INFLATION TO OBSERVABLES: CMB ANISOTROPY

A.1. Introduction

Cosmological perturbation theory during inflation enables to find a connection between the inflationary theory itself and observables represented by the angular distribution of CMB temperature anisotropy.

Let us imagine that CMB photons are coming from a given direction $\vec{n}$ on the celestial sphere and let us call $T_0(\vec{n})$ their temperature. We know, from observational data, that the average value is given by Eq. (2.1). We would like to study the deviation from the average value T_0, i.e. $\delta T_0(\vec{n}) \equiv T_0(\vec{n}) - T_0$, or equivalently the relative temperature fluctuation $\delta T_0(\vec{n})/T_0$.

The equation describing the different physical effects contributing to CMB temperature anisotropy is given by the following *Sachs-Wolfe equation*

$$\frac{\delta T}{T}(\tau_0, \vec{n}) = \frac{1}{4}\delta_\gamma(\tau_{\rm rec}) + \Phi(\tau_{\rm rec}) + \int_{\tau_{\rm rec}}^{\tau_0} d\tau (\Phi' - \Psi') + \vec{n} \cdot \vec{v}(\tau_{\rm rec}) \,, \tag{A.1}$$

where

- $\tau_{\rm rec}$ is the recombination time;
- τ_0 is the present time;
- $\delta_\gamma(\tau_{\rm rec})/4$ accounts for photon density perturbation at the LSS; $\Phi(\tau_{\rm rec})$ describes scalar perturbation of the metric at the LSS. Together, they form the so called *Sachs-Wolfe term*.

- $\int_{\tau_{\rm rec}}^{\tau_0} d\tau(\Phi' - \Psi')$ is the so called *Integrated Sachs-Wolfe effect*: it takes into account the photons' loss of energy when they fall into a gravitational potential in their trajectory towards us.

- $\vec{n} \cdot \vec{v}(\tau_{\rm rec})$ is a Doppler contribution due to the movement of the plasma at the LSS.

Now, let us focus $\delta T_0(\vec{n})/T_0$ as observed today: basically, we are observing a scalar field from a specific frame, which is given essentially by the Earth. So, we are observing a scalar field on a 2-sphere; this let us to expand the relative temperature fluctuation in spherical harmonics, since these form a complete orthonormalised set of functions on a unit sphere. Therefore, we have

$$\frac{\delta T_0}{T_0}(\vec{n}) = \sum_{l=1}^{\infty} \sum_{m=-l}^{l} a_{lm} Y_{lm}(\vec{n}) \tag{A.2}$$

Hence, the coefficients a_{lm} are going to be our observables, in a way. Their magnitude gives us an idea of the amplitude of temperature fluctuations.
Being our Universe isotropic on average, the coefficients a_{lm} satisfy the following relation

$$\langle a_{lm} a^*_{l'm'} \rangle = C_l \, \delta_{ll'} \, \delta_{mm'} \, , \tag{A.3}$$

where

$$C_l = \frac{1}{2l+1} \sum_{m=-l}^{l} \langle a_{lm} a^*_{lm} \rangle \, . \tag{A.4}$$

These coefficients C_l determine completely the CMB temperature anisotropy. Notice that $\langle ... \rangle$ denotes the so called *cosmic average*: we are averaging over an hypotetical ensemble of Universes. Clearly, we have only one Universe where we can perform observations, and a way to elude this problem would be to average over observations of different observers spread throughout our Universe, which is again impossible. The only thing we can do is to consider the relation $\vartheta = \pi/l$ between the angular scale ϑ and the order of the multipole l. For large multipoles, we can divide the surface of the 2-sphere we are observing our Universe from into many little squares of area ϑ^2, so that we have many measurements. There is still a difference between the actual cosmic average and our result which is estimated by $\Delta C_l/C_l \simeq 1/\sqrt{l+1/2}$; as you can see, this relative statistical error decreases as l increases.
These coefficients determine the two-point correlation function of the relative temperature fluctuations, which is eventually given by (for large l)

$$\left\langle \left(\frac{\delta T_0}{T_0}(\vec{n}) \right)^2 \right\rangle \simeq \int d\ln(l) \frac{l(l+1)}{2\pi} C_l \, . \tag{A.5}$$

A useful quantity that characterises temperature fluctuations at a given angular scale l is given by the total angular spectrum

$$\mathscr{D}_l \equiv T_0^2 \frac{l(l+1)}{2\pi} C_l \tag{A.6}$$

To conclude this section, we just give the expression of C_l in terms of the primordial

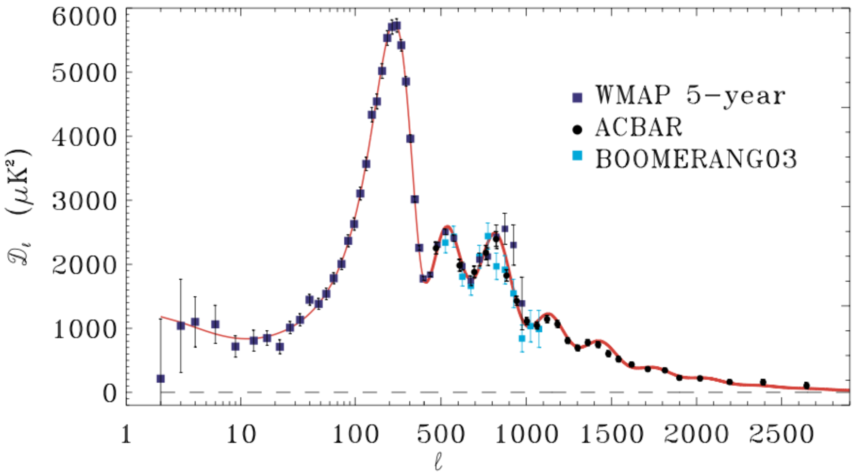

Figure A.1: Behaviour of $\mathscr{D}_l$ as a function of l compared to CMB temperature anisotropy data. The horizontal axis is logarithmic at $l \leq 500$ and linear at higher l.

power spectrum and of the transfer function. Given $\Theta(\vec{n}) \equiv \delta T(\vec{n})/T_0$ and assuming instantaneous recombination[1], we have

$$C_l = 4\pi \int \frac{dk}{k} \mathcal{P}_\Phi(k) \Theta_l^2(k) = \frac{2}{\pi} \int dk\, k^2 P_\Phi(k) \tilde{\Theta}(k) \tilde{\Theta}^*(k) [j_l(kr_*)]^2 \,, \tag{A.7}$$

where $\mathcal{P}_\Phi(k) = k^3 P_\Phi(k)/(2\pi^2)$, with $P_\Phi(k)$ the primordial power spectrum at recombination, whereas $\tilde{\Theta}(k)\tilde{\Theta}^*(k)[j_l(kr_*)]$ is the transfer function. $\tilde{\Theta}$ is defined by the relation $\Theta_l(k) \equiv \tilde{\Theta}(k) j_l(kr_*)$.

Our next goal is to study the behaviour of C_l at different angular scales.

A.2. Large angular scales

First of all, we consider contributions to temperature anisotropy on large angular scale (that is to say low values of l), meaning we are studying perturbations that are superhorizon at recombination (i.e. $k\tau_{\text{rec}} < 1$).

[1] Instantaneous recombination entails that the LSS is located at a constant angular diametral distance from us given by $r = r_*$.

If we assume for the primordial power spectrum the following power law

$$\mathcal{P}_\Phi = A_\Phi \left(\frac{k}{k_*}\right)^{n_s-1}$$

where A_Φ and n_s are respectively the amplitude and the spectral index, then eventually one has

$$C_l^{SW} \simeq \frac{18\pi}{100}\frac{A_\Phi}{l(l+1)}\,, \tag{A.8}$$

for flat primordial power spectrum (i.e. $n_s \simeq 1$). In order to get Eq. (A.8), one neglects the contribution of the ISW effect and of the Doppler term, which are not relevant at these angular scales, as we are going to discuss in a moment. The only contribution we have taken into account is that of the Sachs-Wolfe term. Therefore, if we look at Eq. (A.6), we see how $\mathscr{D}_l$ is independent of l. This mirrors its behaviour for low l in Figure A.1.

Now, let us discuss about the ISW and the Doppler term contribution. First of all, the Doppler term is negligible since it is proportional to the velocity of the baryon-photon component at recombination, and this velocity turns out to be small for superhorizon modes. On the other hand, we can find the ISW contribution and see that it is small except for very low multipoles. To do so, let us neglect the difference between Φ and $(-\Psi)$ in the ISW term inside Eq. (A.1) and let us use the momentum representation to write

$$\Theta^{\rm ISW}(\vec{n}) \simeq 2\int_{\tau_{\rm rec}}^{\tau_0} d\tau \int d^3k\, \Phi'(\tau,\vec{k})e^{i\vec{k}\cdot\vec{n}(\tau_0-\tau)}\,.$$

Under our assumptions, one can use the following expression:

$$\Phi(\tau,\vec{k}) = g(\tau)\frac{9}{10}\Phi(\vec{k},\tau_i)\,,$$

where $\Phi(\vec{k},\tau_i)$ is the gravitational potential at radiation phase, which is constant on superhorizon scales after inflation. We also exploit the expansion of the exponential in terms of Legendre polynomials

$$e^{ix\cos\theta} = \sum_{l=0}^{\infty}(2l+1)(i)^l j_l(x)P_l(\cos\theta)$$

so that

$$\Theta^{ISW}(\vec{n}) = \frac{9}{5}\sum_l \int_{\tau_{\rm rec}}^{\tau_0} d\tau \int d^3k\, g'(\tau)\Phi(\vec{k},\tau_i)i^l(2l+1)j_l[(\tau_0-\tau)k]P_l(\cos\theta)\,.$$

We then compare this result with the expression

$$\begin{aligned}\Theta(\vec{n}) &= \sum_l i^l(2l+1)\int d^3k\,\Theta_l(\vec{k})P_l(\cos\theta)\\ &= \sum_l i^l(2l+1)\int d^3k\,\tilde{\Theta}_l(k)\Phi(\vec{k},\tau_i)P_l(\cos\theta)\,,\end{aligned}$$

(where we have extracted the dependence on the initial gravitational potential via $\Theta_l(\vec{k}) = \tilde{\Theta}_l(k)\Phi(\vec{k},\tau_i)$) to get

$$\tilde{\Theta}_l^{ISW}(k) = \frac{9}{5}\int_{\tau_{\rm rec}}^{\tau_0} d\tau\, g'(\tau)j_l[(\tau_0-\tau)k]\,, \tag{A.9}$$

which is the contribution to the multipole of order l given by modes of momentum k. It is not possible to evaluate the previous integral analytically but we can give an approximate solution. We insert Eq. (A.9) into Eq. (A.7) (use the first equality)

$$\begin{aligned}C_l^{ISW} &= 4\pi\int\frac{dk}{k}\mathcal{P}_\Phi(k)\left(\frac{81}{25}\int_{\tau_{\rm rec}}^{\tau_0} d\tau\, g'(\tau)j_l[(\tau_0-\tau)k]\int_{\tau_{\rm rec}}^{\tau_0} d\tilde{\tau} g'(\tilde{\tau})j_l[(\tau_0-\tilde{\tau})k]\right)\\ &= 4\pi\frac{81}{25}\frac{1}{2\pi^2}\int dk\,k^2P_\Phi(k)\int_{\tau_{\rm rec}}^{\tau_0} d\tau\, g'(\tau)j_l[(\tau_0-\tau)k]\int_{\tau_{\rm rec}}^{\tau_0} d\tilde{\tau} g'(\tilde{\tau})j_l[(\tau_0-\tilde{\tau})k]\,,\end{aligned}$$

where again we have used $\mathcal{P}_\Phi(k) = k^3P_\Phi(k)/(2\pi^2)$. Now we exploit the following approximate formula (which holds only for $l \gtrsim 5$)

$$\int dk\,k^2 f(k)j_l(k\tau)j_l(k\tau') \approx \frac{\pi}{2\tau^2}f\left(\frac{l+1/2}{\tau}\right)\delta(\tau-\tau')\,,$$

with $f(k)$ arbitrary smooth function. Hence

$$\begin{aligned}C_l^{ISW} &\approx 4\frac{81}{100}\int_{\tau_{\rm rec}}^{\tau_0} d\tau\int_{\tau_{\rm rec}}^{\tau_0} d\tilde{\tau}\, g'(\tau)g'(\tilde{\tau})P_\Phi\left(\frac{l+1/2}{\tau_0-\tau}\right)\frac{1}{(\tau_0-\tau)^2}\delta[(\tau_0-\tau)-(\tau_0-\tilde{\tau})]\\ &= 4\frac{81}{100}\int_{\tau_{\rm rec}}^{\tau_0} d\tau\left(\frac{g'(\tau)}{\tau_0-\tau}\right)^2 P_\Phi\left(\frac{l+1/2}{\tau_0-\tau}\right)\end{aligned} \tag{A.10}$$

We then proceed with a change of integration variable from τ to $\xi = \tau/\tau_0$. Furthermore, in the case at hand we have

$$\mathcal{P}_\Phi = A_\Phi\left(\frac{k}{k_*}\right)^{n_s-1} = A_\Phi\left(\frac{l+1/2}{k_*(\tau_0-\tau)}\right)^{n_s-1}\,,$$

so that

$$\begin{aligned}
P_\Phi &= \left(\frac{\tau_0-\tau}{l+1/2}\right)^3 2\pi^2 A_\Phi \left(\frac{l+1/2}{k_*(\tau_0-\tau)}\right)^{n_s-1} \\
&= 2\pi^2 (l+1/2)^{n_s-4} A_\Phi \left(\frac{1}{k_*(\tau_0-\tau)}\right)^{n_s-1} (\tau_0-\tau)^3 \\
&= 2\pi^2 \tau_0^3 (1-\xi)^3 A_\Phi (l+1/2)^{n_s-4} \left(\frac{1}{k_*(\tau_0-\tau)}\right)^{n_s-1} . \qquad \text{(A.11)}
\end{aligned}$$

By inserting Eq. (A.11) inside Eq. (A.10) with the previous change of variable, we get

$$\begin{aligned}
C_l^{ISW} &\approx 8\pi^2 \frac{81}{100} A_\Phi \left(l+\frac{1}{2}\right)^{n_s-4} \int_{\frac{\tau_{\rm rec}}{\tau_0}}^1 d\xi \left[\tau_0^4 \left(\frac{\partial g}{\partial \xi}\right)^2 \left(\frac{\partial \xi}{\partial \tau}\right)^2 \left(\frac{1}{\tau_0}\right)^2 \left(\frac{1}{1-\xi}\right)^2 \times \right. \\
&\qquad \left. \times \frac{1}{k_*^{n_s-1}} \frac{1}{\tau_0^{n_s-1}} \frac{(1-\xi)^3}{(1-\xi)^{n_s-1}} \right] \\
&= 8\pi^2 \frac{81}{100} A_\Phi \left(\frac{1}{k_*\tau_0}\right)^{n_s-1} \left(l+\frac{1}{2}\right)^{n_s-4} \int_{\frac{\tau_{\rm rec}}{\tau_0}}^1 d\xi \, (1-\xi)^{2-n_s} \left(\frac{\partial g}{\partial \xi}\right)^2 .
\end{aligned}$$

For flat Primordial Power Spectrum ($n_s = 1$)

$$C_l^{ISW} \approx 8\pi^2 \frac{81}{100} \frac{A_\Phi}{(l+1/2)^3} \int_{\frac{\tau_{\rm rec}}{\tau_0}}^1 d\xi \, (1-\xi) \left(\frac{\partial g}{\partial \xi}\right)^2 . \qquad \text{(A.12)}$$

From Eqs.(A.12) and (A.6) we can see how the contribution to $\mathscr{D}_l$ of the ISW effect decays when l increases, i.e. for large angular scales. This is the reason why we had neglected its contribution to get the result in Eq. (A.8).

Actually, the ISW contribution becomes relevant only for the lowest multipoles. To see this, we first consider a numerical solution to Eq. (A.12) given by

$$C_l^{ISW} \simeq 1.2 \cdot \frac{A_\Phi}{(l+1/2)^3} . \qquad \text{(A.13)}$$

Then, we compare Eq. (A.13) to Eq. (A.8) and we get

$$\frac{C_l^{ISW}}{C_l^{SW}} \simeq 2.17 \cdot \frac{l(l+1)}{(l+1/2)^3} \qquad \text{(A.14)}$$

As we can see from Eq. (A.14), the two contributions are comparable only for l very small, i.e. for the lowest multipoles, as we were saying before. Furthermore, this result is in agreement with what is shown in Figure A.2.

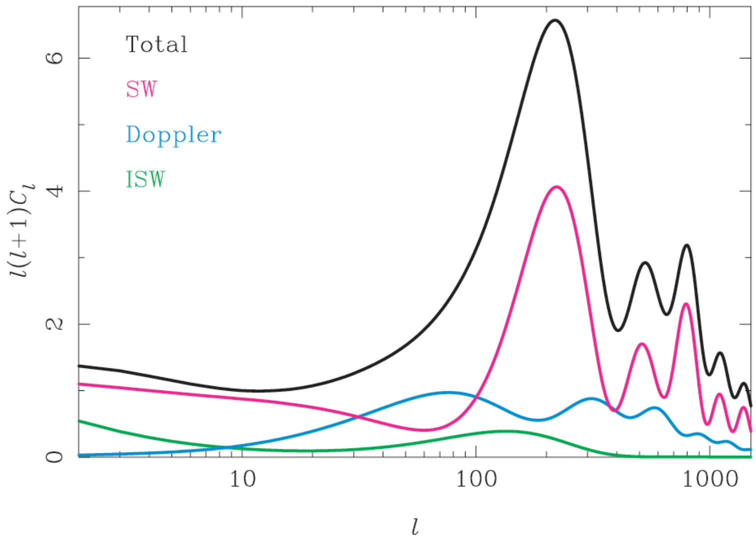

Figure A.2: Different contributions to temperature anisotropy.

A.3. Intermediate angular scales

Let us now consider the contribution of perturbations at intermediate angular scales; in terms of angular armonics we have

$$l \lesssim 1000\,,$$

i.e. $k\tau_{\rm rec} \gtrsim 1$. As for the previous section, we are going to analyse the contribution to temperature anisotropy given by the SW, Doppler and ISW terms, neglecting the interference among them, which will be discussed later.
Let us begin with the SW term: avoiding mathematical details, the contribution to the multipoles $\Theta_l(\vec{k})$ coming from the SW term is given by

$$\Theta_l^{SW}(\vec{k}) = \left(\Phi(\tau_{\rm rec}) + \frac{1}{4}\delta_\gamma(\tau_{\rm rec})\right) j_l[k(\tau_0 - \tau_{\rm rec})]\,, \tag{A.15}$$

where the expression inside round brackets turns out to be

$$\Phi(\tau_{\rm rec}) + \frac{1}{4}\delta_\gamma(\tau_{\rm rec}) = \{A(\tau_{\rm rec})\cos[kr_s(\tau_{\rm rec})] - B(k,\tau_{\rm rec})\}\,\Phi(k,\tau_i) \tag{A.16}$$

with $A(\tau)$ and $B(k,\tau)$ positive functions slowly varying in time, and

$$r_s(\tau) = \int_0^\tau \frac{d\bar{\tau}}{\sqrt{3(1+R_B(\bar{\tau}))}}\,, \qquad R_B = \frac{3\rho_B}{4\rho_\gamma}$$

We can already see from Eq. (A.15) that there is an oscillating contribution to the angular spectrum. However, the actual SW contribution is determined by C_l, which contains the quantity Θ_l^{SW} squared, which means that the position of the maxima in C_l are given by the position of both maxima and minima of the cosine in Θ_l^{SW}. Eventually, the computation of C_l^{SW} yields

$$\begin{aligned} C_l^{SW} = \frac{2\pi}{l^2} A_\Phi \bigg\{ &\frac{1}{2} c_1 A^2 + \frac{8}{15} c_2 B^2 \\ &+ \int_1^\infty \frac{du}{u^2\sqrt{u^2-1}} \left[\frac{1}{2} A^2 \cos\left(2\frac{lr_s}{\tau_0}u\right) - 2AB\cos\left(2\frac{lr_s}{\tau_0}u\right)\right]\bigg\} , \end{aligned} \tag{A.17}$$

where c_1 and c_2 are constants of order 1, and $u = k\tau_0/l$. The first two terms are monotonically decreasing with l, whereas the integral is responsible for the oscillatory behaviour of C_l^{SW}. We can give an estimate as follows: the integral is saturated in a region close to $u = 1$, where $u^{-2} \simeq 1$ and $\sqrt{u^2-1} \simeq \sqrt{2}\sqrt{u-1}$. With this at hand, we can exploit the know integral

$$\int_1^\infty \frac{du}{\sqrt{u-1}} \cos(\alpha u) = \sqrt{\frac{\pi}{\alpha}} \cos\left(\alpha + \frac{\pi}{4}\right)$$

in order to write

$$\begin{aligned} &\int_1^\infty \frac{du}{u^2\sqrt{u^2-1}} \left[\frac{1}{2} A^2 \cos\left(2\frac{lr_s}{\tau_0}u\right) - 2AB\cos\left(2\frac{lr_s}{\tau_0}u\right)\right] \\ &\quad \simeq \sqrt{\frac{\pi l^{(r)}}{2l}} \left[\frac{1}{2\sqrt{2}} A^2 \cos\left(2\frac{l}{l^{(r)}} + \frac{\pi}{4}\right) - 2AB\cos\left(\frac{l}{l^{(r)}} + \frac{\pi}{4}\right)\right] , \end{aligned} \tag{A.18}$$

where we have defined $l^{(r)} \equiv \tau_0/r_s$.

Now let us study the contribution of the Doppler term, given by

$$\Theta_l^D(\vec{k}) = -kv_B(\tau_{\rm rec}) j_l'[k(\tau_0 - \tau_{\rm rec})] \tag{A.19}$$

where the prime refers to the derivative of the spherical Bessel function with respect to its argument and $kv_B(\tau)$ is called "photon density contrast" and is given by

$$kv_B(\tau) = -3u_s \Phi(k,\tau_i) A(k,\tau) \sin\left(k \int_0^\tau \frac{d\bar{\tau}}{\sqrt{3(1+R_B(\bar{\tau}))}}\right) \tag{A.20}$$

with

$$3u_s \equiv \frac{\sqrt{3}}{1+R_B(\tau_{\rm rec})} .$$

The computation of the coefficient C_l^D, assuming flat primordial power spectrum, yields

$$C_l^D = \frac{2\pi}{l^2} A_\Phi \left[\frac{3u_s}{2} c_3 A^2 - \int_1^\infty du \, \frac{\sqrt{u^2-1}}{u^4} \frac{(3u_s)^2}{2} A^2 \cos\left(2\frac{l}{l^{(r)}} u \right) \right] \tag{A.21}$$

where c_3 is again a constant of order 1. Once more, we would like to give an estimate of the oscillatory behaviour. Since the argument of the integral in Eq. (A.21) is small where $u \simeq 1$, the oscillating part is suppressed by the factor $l^{(r)}/l$. Thus, we integrate by parts setting $A \approx$ const. and we get to the leading order in $l^{(r)}/l^2$

$$\begin{aligned} -\int_1^\infty du \, \frac{\sqrt{u^2-1}}{u^4} \frac{(3u_s)^2}{2} A^2 \cos\left(2\frac{l}{l^{(r)}} u \right) \\ \simeq \frac{(3u_s)^2}{2} A^2 \frac{l^{(r)}}{2l} \int_1^\infty \frac{du}{u^3 \sqrt{u^2-1}} \sin\left(2\frac{l}{l^{(r)}} u \right) . \end{aligned}$$

Near $u \simeq 1$ we can consider $u^{-3} \simeq 1$ and $\sqrt{u^2-1} \simeq \sqrt{2}\sqrt{u-1}$ and finally we get

$$\begin{aligned} -\int_1^\infty du \, \frac{\sqrt{u^2-1}}{u^4} \frac{(3u_s)^2}{2} A^2 \cos\left(2\frac{l}{l^{(r)}} u \right) \\ \simeq \frac{(3u_s)^2}{4} A^2 \frac{l^{(r)}}{l} \frac{1}{\sqrt{2}} \sqrt{\frac{\pi l^{(r)}}{2l}} \cos\left(2\frac{l}{l^{(r)}} - \frac{\pi}{4} \right) \\ = \frac{(3u_s)^2 l^{(r)}}{2l} \frac{A^2}{4} \sqrt{\frac{\pi l^{(r)}}{l}} \cos\left(2\frac{l}{l^{(r)}} - \frac{\pi}{4} \right) . \end{aligned} \tag{A.22}$$

Let us just briefly mention what happens for the ISW effect. Here the only contribution is due to the *early ISW effect.*[3] This is relevant for $k\tau_{\text{rec}} \sim 1$ which lies exactly in our region, in particular near the first peak in Fig. A.2. However, its contribution to C_l turns out to be suppressed by the factor

$$\left(\frac{\rho_{\text{rad}}}{\rho_M} (\tau_{\text{rec}}) \right)^2 \simeq 0.12 \, .$$

Finally, let us quickly discuss how there is interference between the different contributions to temperature anisotropy. To begin with, let us recall that the total anisotropy is given by the integral over momenta of $\left| \Theta_l^{SW}(\vec{k}) + \Theta_l^{ISW}(\vec{k}) + \Theta_l^D(\vec{k}) \right|^2$: therefore, it is clear from this expression that we have interference between the different pieces. In particular, if we look at the expression of the ISW contribution to

[2] Remember that A is a function of $k = l/\tau_0$ so it can be seen as a function of l as well.

[3] People distinguish between the early ISW effect, which takes place just after recombination, and late ISW effect, which is due to the fact that $\Omega_m \simeq 0.3$, meaning that there is presence of dark matter and dark energy in the model at hand.

the multipoles

$$\Theta_l^{ISW}(\vec{k}) = \frac{1}{l\sqrt{u}(u^2-1)^{1/4}} \times \\ \times \left\{ \cos\left[\left(l+\frac{1}{2}\right)\phi(u)\right] I_c^{ISW} + \sin\left[\left(l+\frac{1}{2}\right)\phi(u)\right] I_s^{ISW} \right\}, \quad \text{(A.23)}$$

where

$$\phi(u) = \sqrt{u^2-1} - \arccos\left(\frac{1}{u}\right) - \frac{\pi}{4}$$
$$I_c^{ISW} = 2\int_{\tau_{\mathrm{rec}}}^{\tau_0} d\tau\, \Phi' \cos\left(l\frac{\tau}{\tau_0}\sqrt{u^2-1}\right)$$
$$I_s^{ISW} = 2\int_{\tau_{\mathrm{rec}}}^{\tau_0} d\tau\, \Phi' \sin\left(l\frac{\tau}{\tau_0}\sqrt{u^2-1}\right),$$

we have that the oscillating terms in Eq. (A.23) associated with I_c^{ISW} and I_s^{ISW} have the same phase as $j_l[k(\tau_0-\tau_{\mathrm{rec}})]$ and $j_l'[k(\tau_0-\tau_{\mathrm{rec}})]$ (in Eqs. (A.15) and (A.19)) respectively, meaning that those terms interfere with the SW and the Doppler effect.

A.4. Small angular scales

Our last topic is the discussion of the behaviour of temperature anisotropy at small angular scales ($l \gtrsim 1000$). The point here is that we have to give up two assumptions, i.e. the instantaneous photon decoupling and the tight coupling approximation. [4]We must consider at least four important effects that we are going to list:

1. The Silk damping.
2. The finite thickness of the Last Scattering Surface.
3. The weak gravitational lensing.[5]
4. The Sunyaev-Zeldovich effect.

The first two take place during recombination and last scattering epoch respectively. In addition, structures in the late Universe are responsible for the modification of the

[4]Due to intense scattering of photons off electrons and Coulomb interactions between electrons and baryons, the baryon-photon plasma is considered to be a single medium, meaning that the velocities of baryons and photons coincide.

[5]In GR we distinguish among three different categories of lensing: strong, weak and microlensing. Strong lensing occurs when the source and the gravitational lens are relatively close to each other; moreover, in order to have strong lensing, two conditions must be satisfied: the lens must be very massive and the source must be almost exactly behind the lens. Strong lensing is responsible for extreme distortion of the light coming from the source. On the other hand, weak lensing still requires a massive lens, but it is not necessary for the source to be exactly behind the lens. The distortion is not as large as in strong lensing. Finally, microlensing is a kind of lensing where the brightness of the source changes when it passes behind a small object which behaves as a lens.

CMB spectrum at small angular scales and this is encoded in the last two effects, which generate a so called *secondary anisotropy*: with this terminology we mean that the phenomenon acting on CMB photons does not take place at the LSS. In the case at hand, for instance, CMB photons just feel the presence of structure in the late Universe.

A.4.1 The Silk damping

Let us begin with the discussion of the Silk damping. This effect takes place during recombination and deals with the suppression of acoustic oscillations in the baryon-photon plasma. Basically, during recombination we have few free electrons and the mean free path of photons is very large. Even when they scatter off electrons, there is no change in photons' energy so that they can travel from overdense regions to underdense regions, transferring their energy in such a way that they remove density fluctuations.

When one translates this into a mathematical language, the result is a suppression factor for acoustic oscillations of perturbations of momentum k of the kind $e^{-(k/k_S)^2}$ where $k_S \equiv k_S(\tau_{\rm rec}) \sim a_0 \cdot 0.1 \mathrm{Mpc}^{-1}$. This factor goes along with the oscillating parts we have seen in the previous section. Since those oscillating parts are related to δ_γ and v_γ squared, the actual damping factor is $e^{-2(k/k_S)^2} = e^{-(l/l_S)^2}$, where

$$l_S = \frac{k_S \tau_0}{\sqrt{2}} \sim 1000$$

so that the suppression becomes relevant already at $l \gtrsim l_S$. Basically, the main effect introduced by the Silk damping is the replacement of the amplitude A in Eqs. (A.17) and (A.21) with $A \cdot e^{-\frac{l}{2 l_S}}$.

On top of that, there is still the non-oscillating part of perturbations, represented by the amplitude B in Eq. (A.17), which is not affected by the Silk damping. However, the dependence of B on k is such that

$$B \sim \frac{1}{k^2}$$

so that the whole angular anisotropy decreases with l for $l \gtrsim 1000$.

A.4.2 The finite thickness of the LSS

So far, we have assumed that photons decoupled instantaneously after recombination, but actually the sphere of last scattering has a finite width, bringing about a further damping. Let us give an approximate description of this phenomenon.

If we reject the simultaneous decoupling, then we shall consider different times τ_j

at which photons last scattered. From a mathematical perspective, this entails that the functions $\Phi(\tau_{\rm rec})$, $\delta_\gamma(\tau_{\rm rec})$ and $v_\gamma(\tau_{\rm rec})$ are replaced by convolutions with a so called *visibility function*. Leaving aside technical details, this function can be approximated by a Gaussian in τ_j centered at $\tau_j = \tau_{\rm rec}$ with width $\Delta\tau_{\rm rec}$.
For example, let us consider the pure SW term: for a perturbation of momentum $\vec{k}$ to temperature anisotropy in the direction $\vec{n}$, one has

$$\Theta(\vec{k}\cdot\vec{n}, k) = \int d\tau_j \, N \, e^{\frac{-(\tau_j-\tau_{\rm rec})^2}{2\Delta\tau_{\rm rec}^2}} \, e^{i\vec{k}\cdot\vec{n}(\tau_0-\tau_j)} \left\{A\cos[kr_s + ku_s(\tau_j - \tau_{\rm rec})] - B\right\} \Phi(\vec{k}, \tau_i)\,,$$

where N is a normalisation factor for the Gaussian. Given that A and B are slowly varying functions in the variable τ, one can set $A = A(\tau_{\rm rec})$ and $B = B(\tau_{\rm rec})$. Upon solving the integral, the final expression would be

$$\begin{aligned}\Theta(\vec{k}\cdot\vec{n}, k) = e^{i\vec{k}\cdot\vec{n}(\tau_0-\tau_{\rm rec})} \Bigg\{ \frac{A}{2} \Bigg[& e^{-\frac{\Delta\tau_{\rm rec}^2}{2}(\vec{k}\cdot\vec{n}-ku_s)^2} e^{ikr_s} \\ & + e^{-\frac{\Delta\tau_{\rm rec}^2}{2}(\vec{k}\cdot\vec{n}-ku_s)^2} e^{-ikr_s} \Bigg] - e^{-\frac{\Delta\tau_{\rm rec}^2}{2}(\vec{k}\cdot\vec{n})^2} B \Bigg\} \Phi(\vec{k}, \tau_i)\,.\end{aligned} \tag{A.24}$$

Eq. (A.24) shows that the finite thickness of the LSS generally brings about an exponential suppression which however depends on the direction of propagation of the perturbation. Perturbations associated with B undergo no suppression if they propagate normally to the line of sight. This finds an explanation if we recall that B is a slowly varying function in the argument τ; thus, if it depends weakly on time, perturbations with momenta normal to the line of sight essentially look the same along the line of sight in the interval $\Delta\tau_{\rm rec}$.
Also, perturbations related to A are not suppressed for particular directions (i.e. those such that $\vec{k}\cdot\vec{n} - ku_s = 0$). However, this is not the case for the oscillating terms in Eq. (A.17), for which $\vec{k}\cdot\vec{n} \sim \frac{1}{l} \ll 1$. Therefore, the associated suppression factor is

$$C_l^{(\rm osc)} \propto e^{-(ku_s\Delta\tau_{\rm rec})^2} = e^{-\frac{l^2}{\Delta l^2}}\,, \tag{A.25}$$

where

$$\Delta l = \frac{\tau_0}{u_s\Delta\tau_{\rm rec}} \simeq 2800\,. \tag{A.26}$$

Eqs. (A.25) and (A.26) show that, on top of the Silk damping, there is a strong suppression of oscillations in the angular spectrum for $l \gtrsim 2800$ due to the finite thickness of the LSS.

A.4.3 The weak gravitational lensing and the Sunyaev-Zeldovich effect

Structures in the late Universe like galaxies or cluster of galaxies can slightly deflect CMB photons due to weak gravitational lensing. As small as it may be, this effect must be taken into account at small angular scales since it generates secondary anisotropy.
Finally, let us discuss the Sunyaev-Zeldovich effect. It is still due to cluster of galaxies which are rich in hot ionized gas: in fact, when CMB photons pass through clusters, they can scatter off hot electrons. As a result, the photons are heated up. Therefore, not only they generate a secondary anisotropy, but they also modify the Planck spectrum when we look at it the direction of the clusters themselves, since those photons basically move from lower to higher frequencies. By the way, the frequency signature of this effect enabled the development of new techniques to study clusters of galaxies.

A.5. Conclusions

First of all, the analysis performed for large angular scales ($l \lesssim 20$) has shown how the actual contribution to temperature anisotropy comes from the pure SW term inside Eq. (A.1): the Doppler term is negligible due to the small value of the velocity of the baryon-photon component; on the other hand, the effect of the ISW term is negligible with respect to the pure SW term as shown by Eq. (A.14), even though the ISW effect achieves its highest value only for very large angular scales (i.e. for $l \to 0$) as we can clearly see from Eq. (A.13).
We have then moved to the study of intermediate angular scales, where Eqs. (A.18) and (A.22) show a clear oscillating behaviour of the SW and Doppler contribution respectively. Moreover, if we compare Eq. (A.20) to (A.16) we see that the phase of oscillation is shifted by $\pi/2$. Hence, the maxima of the Doppler contribution to C_l are shifted with respect to the maxima of the SW contribution, and this is exactly what is observed in Figure A.2. We also notice that the oscillatory pattern of the spectrum in Figure A.2 is dominated by the SW part, in spite of the fact that its original magnitude is comparable to the one associated with the Doppler effect (see respectively Eqs. (A.16) and (A.20)). To explain this, one should recall the fact that the Doppler contribution of a perturbation with momentum $\vec{k}$ is proportional to the projection of the velocity on the line of sight, that is to say to $\vec{n} \cdot \vec{n}_k = \cos\theta$. This means that the oscillations associated with the Doppler effect are partially removed. As far as the ISW effect is concerned, we have seen that only the early ISW part has to be considered, even though it is small and it is present only close to the first

peak. Also, Eq. (A.23) decays for large values of l, showing how the ISW effect gives no contribution for higher l.

Finally, we have investigated what happens for small angular scales. We have seen how there is a general suppression of the multipoles due to four differen effects, two of which related to recombination and the finite thickness of the LSS, whereas the other two are connected to structures in the late Universe. Once again, there is concordance between what we have discussed and Figure A.1.

To sum up, the study we have carried out reproduces the behaviour of the angular spectrum of temperature anisotropy: first of all, for large angular scales the main contribution is given by the SW effect; in particular, Eq. (A.13) makes sure that, for low values of l, the angular spectrum is basically flat, and this is where the so called *Sachs-Wolfe plateau* in Figure A.1 comes from. Then, the oscillating behaviour of the angular spectrum at intermediate angular scales is provided essentially by the SW, the Doppler term, and by the interference between them and the ISW term. This is the reason why we observe the *acoustic peaks* in Figure A.1. Furthermore, all of these contributions decay when l increases, and this is another feature of the angular spectrum we can find in Figure A.1. Finally, the oscillations and the whole angular spectrum are quickly suppressed as we move to small angular scales ($l \gtrsim 1000$), and this is in agreement with our discussion in Section A.4.

APPENDIX B

ABOUT SCALAR FIELD COSMOLOGY WITH AN EXPONENTIAL POTENTIAL

B.1. Autonomous system for a FLRW cosmology with an exponential potential

We shall derive the autonomous system (3.6)-(3.7) containing the evolution equation for a FLRW cosmology with a scalar field featured by an exponential potential. First of all, we derive an expression for $\dot{H}$ we are going to use in a while. We take the derivative with respect to time of Eq. (2.27):

$$2H\dot{H} = \frac{1}{3M_P^2}\left(\dot{\phi}\ddot{\phi} + \frac{dV}{dt}\right) .$$

Considering the potential (3.1) and keeping in mind that we are assuming an homogeneous scalar field $\phi = \phi(t)$, we have

$$\frac{dV}{dt} = -\frac{\lambda\dot{\phi}}{M_P}V(\phi) ,$$

so that

$$\dot{H} = \frac{\dot{\phi}}{6M_P^2 H}\left(\ddot{\phi} - \frac{\lambda}{M_P}V\right) .$$

Then, we exploit the KG equation (2.26) for $\ddot{\phi}$ in order to get

$$\dot{H} = \frac{\dot{\phi}}{6M_P^2 H}\left(-3H\dot{\phi} - \partial_\phi V - \frac{\lambda}{M_P}V\right).$$

Given $-\partial_\phi V = V\lambda/M_P$, we have

$$\dot{H} = \frac{\dot{\phi}}{6M_P^2 H}\left(-3H\dot{\phi} + \frac{\lambda}{M_P}V - \frac{\lambda}{M_P}V\right) = -\frac{\dot{\phi}^2}{2M_P^2}. \tag{B.1}$$

Considering the definition (3.3) of the dimensionless variable x, we finally get

$$\dot{H} = -3x^2H^2. \tag{B.2}$$

Next, we shall see how to get the autonomous system. To begin with, we invert Eq. (3.3) so that $\dot{\phi} = \sqrt{6}M_P Hx$, and we compute the second derivative of ϕ with respect to time:

$$\ddot{\phi} = \sqrt{6}M_P(\dot{H}x + H\dot{x}).$$

Recalling the relation (2.31) and using Eq. (B.2), we have

$$\ddot{\phi} = \sqrt{6}M_P\left(-3H^2x^3 + H^2x'\right), \tag{B.3}$$

where a prime denotes a derivative with respect to the number of e-foldings. We then invert Eq. (B.1) so as to get an expression for $\dot{\phi}$ and we plug it inside the KG equation (2.26), along with Eq. (B.3), yielding

$$\sqrt{6}M_P\left(-3x^3H^2 + H^2x'\right) + 3H^2\sqrt{6}M_P x + \partial_\phi V = 0.$$

We use again $\partial_\phi V = V(-\lambda)/M_P$. Thus,

$$\sqrt{6}M_P H^2\left[(-3x^3 + x') + 3x\right] - \frac{\lambda}{M_P}V = 0,$$

i.e.

$$x' = -3x(1-x^2) + \lambda\frac{V}{\sqrt{6}M_P^2H^2}.$$

From the definition (3.4) of the dimensionless variable y we get $y^2 = \pm V/(3M_P^2H^2)$, where the $\pm$ accounts for the possibility for V of being positive or negative. Hence we get the first equation of the autonomous system

$$x' = -3x(1-x^2) \pm \lambda\sqrt{\frac{3}{2}}y^2.$$

The next step is the derivation of the equation for the variable y. Considering once again the relation (2.31), we write

$$y' = \frac{1}{H}\dot{y} = \frac{1}{H}\left(-\frac{\sqrt{|V|}}{\sqrt{3}M_P H^2}\dot{H} + \frac{1}{\sqrt{3}M_P H}\frac{1}{2\sqrt{|V|}}\frac{d|V|}{dt}\right) .$$

Using Eqs. (B.2) and (3.4) we have

$$y' = 3x^2 y + \frac{1}{\sqrt{3}M_P H^2}\frac{1}{2\sqrt{|V|}}\frac{|V|}{V}\frac{dV}{dt} .$$

The time derivative of V is $\dot{V} = -\dot{\phi}\lambda V/M_P$, so that

$$y' = 3x^2 y + \frac{1}{\sqrt{3}M_P H^2}\frac{1}{2}\sqrt{|V|}\frac{1}{V}\left(-\lambda V\frac{\dot{\phi}}{M_P}\right) .$$

Combining Eqs. (B.2) and (B.1), we have $\dot{\phi} = \sqrt{6}M_P x H$, which we plug into the previous expression in order to get

$$y' = 3x^2 y - \lambda\frac{\sqrt{|V|}}{\sqrt{3}M_P H}\frac{1}{\sqrt{2}}\sqrt{3}x = 3x^2 y - \lambda\sqrt{\frac{3}{2}}xy$$

i.e.

$$y' = xy\left(3x - \lambda\sqrt{\frac{3}{2}}\right)$$

which is the second equation of the autonomous system.

BIBLIOGRAPHY

[1] D. Baumann, *The Physics of Inflation. A Course for Graduate Students in Particle Physics and Cosmology*, Institute of Theoretical Physics, University of Amsterdam.

[2] R. G. Cai, J. Y. Ji and K. S. Soh, Phys. Rev. D **57** (1998) 6547 [arXiv:gr-qc/9708063].

[3] K. C. K. Chan, J. H. Horne and R. B. Mann, Nucl. Phys. B **447** (1995) 441 [arXiv:gr-qc/9502042].

[4] E. J. Copeland, A. R. Liddle and D. Wands, Phys. Rev. D **57**, (1998) 4686

[5] J. K. Erickson, D. H. Wesley, P. J. Steinhardt and N. Turok, Phys. Rev. D **69** (2004) 063514.

[6] F. Finelli and A. Gruppuso, *Notes for static spherically symmetric solution with an exponential potential*, unpublished

[7] D. J. Fixsen, Astrophys. J. **707** (2009) 916-920.

[8] A. Frolov and L. Kofman, JCAP **0305** (2003) 009

[9] D. S. Gorbunov and V. A. Rubakov, *Introduction to the Theory of the Early Universe - Hot Big Bang Theory*, World Scientific (2011).

[10] D. S. Gorbunov and V. A. Rubakov, *Introduction to the Theory of the Early Universe - Cosmological Perturbations and Inflationary Theory*, World Scientific (2011).

[11] Z. K. Guo, Y. S. Piao and Y. Z. Zhang, Phys. Lett. B **576** (2003) 12-17.

[12] J. C. Hamilton, J. M. Le Goff., P. Ntelis et al. , JCAP **06** (2017)

[13] I. P. C. Heard and D. Wands, Class. Quant. Grav. **19** (2002) 5435-5448.

[14] A. R. Liddle and S. M. Leach, Phys. Rev. D **68** (2003) 103503

[15] T. Matos, F. S. Guzman and D. Nunez, Phys. Rev. D **62** (2000) 061301 [arXiv:astro-ph/0003398].